TECHNICAL REPORT STANDARD PAGE

1. Report No.	2. Government Accession No.	3. Recipients Catalog No.
FHWA/LA-94/288		

4. Title and Subtitle	5. Report Date
Determination of Significant Factors Controlling Compatibility of Asphalts with Synthetic Polymers	June 1995
	6. Performing Organization Code
7. Authors	8. Performing Organization Report No.
William H. Daly, John R. Collier, Ioan I. Negulescu, Zhaoyao Qiu (Chiu), Jane Runkle	
9. Performing Organization Name and Address	10. Work Unit No.
Departments of Chemistry and Chemical Engineering Louisiana State University Baton Rouge, LA 70803	90-1B
	11. Contract or Grant No.
12. Sponsoring Agency Name and Address	13. Type of Report and Period Covered
Louisiana Department of Transportation and Development P.O. Box 94245 Baton Rouge, LA 70804-9245	Final Report August 1989 - June 1992
	14. Sponsoring Agency Code

15. Supplemental Notes

Conducted in cooperation with the U.S. Department of Transportation, Federal Highway Administration
NCP No. 4E1F4011

16. Abstract

The primary objective of this work is to evaluate several significant factors controlling compatibility between asphalt and synthetic polymers. Employing NMR, FTIR, differential scanning calorimetry (DSC), dynamic mechanical spectrometry(DMS) and thermomechanical analysis (TMA) techniques, we have determined the composition and crystallinity of representative asphalts along with their dynamic physical properties. Eight asphalt samples from four manufacturers with grades from AC-10 to AC-30 were characterized by penetration, viscosity, temperature sensitivity, ^{13}C NMR, FTIR, dynamic mechanical analysis (DMA) and DSC. Glass transition temperatures (T_g) and activation energies for the relaxation process of the asphalt were determined with DMA experiments. The crystallizable component of the asphalt was measured with DSC, and polar groups in the asphalt were analyzed with FTIR.

Techniques for slightly chlorinating polyethylene to improve its compatibility with asphalt are reported. Both HDPE and chlorinated polyethylene (CPE) modified asphalts containing 5 wt% polymer were studied using classical techniques and dynamic mechanical analysis (DMA) in both bending mode and shear mode. DSC, fluorescence reflection microscopy and FTIR were also employed to characterize the polymer modified asphalts. Penetration, viscosity, creep resistance and low temperature crack resistance of the asphalt and the polymer modified asphalts were evaluated. The results confirm that CPEs with low chlorine contents (<15 wt %) are more compatible with asphalt than HDPE and, therefore, exhibit better reinforcement effects in asphalt cements. Constant stress creep and 50 Hz dynamic crack resistance are excellent tests for determining polymer-asphalt compatibility.

17. Key Words	18. Distribution Statement
Asphalt/HDPE, asphalt/CPE blends, CPE preparation, DSC, Tg, creep resistance, low temperature crack resistance, compatibility	

19. Security Classification (of this report)	20. Security Classification (of this page)	21. No. of Pages	22. Price
None	None	74	N/A

Form DOT F 1700.7 (8-69)

DETERMINATION OF SIGNIFICANT FACTORS CONTROLLING COMPATIBILITY OF ASPHALT WITH SYNTHETIC POLYMERS

FINAL REPORT

by

WILLIAM H. DALY
PROFESSOR OF CHEMISTRY

JOHN R. COLLIER
PROFESSOR OF CHEMICAL ENGINEERING

IOAN I. NEGULESCU
ASSOCIATE PROFESSOR OF CHEMISTRY, RESEARCH

ZHAOYAO QIU (CHIU)
GRADUATE STUDENT IN CHEMISTRY

JANE RUNKLE
GRADUATE STUDENT IN CHEMICAL ENGINEERING

LOUISIANA STATE UNIVERSITY
BATON ROUGE, LA 70803

CONDUCTED FOR

LOUISIANA DEPARTMENT OF TRANSPORTATION AND DEVELOPMENT
LOUISIANA TRANSPORTATION RESEARCH CENTER
in cooperation with
U. S. DEPARTMENT OF TRANSPORTATION
FEDERAL HIGHWAY ADMINISTRATION

The contents of this report reflect the views of the authors, who are responsible for the facts and the accuracy of the data presented herein. The contents do not necessarily reflect the official views or policies of the Louisiana Transportation Research Center, the Louisiana Department of Transportation and Development or the Federal Highway Administration. The report does not constitute a standard, specification or regulation.

JUNE 1995

ABSTRACT

The primary objective of this work is to evaluate several significant factors controlling compatibility between asphalt and synthetic polymers. Employing NMR, FTIR, differential scanning calorimetry (DSC), dynamic mechanical spectrometry(DMS) and thermomechanical analysis (TMA) techniques, we have determined the composition and crystallinity of representative asphalts along with their dynamic physical properties. Eight asphalt samples from four manufacturers with grades from AC-10 to AC-30 were characterized by penetration, viscosity, temperature sensitivity, ^{13}C nmr, FTIR, dynamic mechanical analysis (DMA) and DSC. Glass transition temperatures (T_g) and activation energies for the relaxation process of the asphalt were determined with DMA experiments. The crystallizable component of the asphalt was measured with DSC, and polar groups in the asphalt were analyzed with FTIR.

Techniques for slightly chlorinating polyethylene to improve its compatibility with asphalt are reported. Both HDPE and chlorinated polyethylene (CPE) modified asphalts containing 5 wt% polymer were studied using classical techniques and dynamic mechanical analysis (DMA) in both bending mode and shear mode. DSC, fluorescence reflection microscopy and FTIR were also employed to characterize the polymer modified asphalts. Penetration, viscosity, creep resistance and low temperature crack resistance of the asphalt and the polymer modified asphalts were evaluated. The results confirm that CPEs with low chlorine contents (<15 wt %) are more compatible with asphalt than HDPE and, therefore, exhibit better reinforcement effects in asphalt cements. Constant stress creep and 50 Hz dynamic crack resistance are excellent tests for determining polymer-asphalt compatiblity.

IMPLEMENTATION STATEMENT

This study encompassed exploratory work to examine the factors controlling compatility between asphalt cement and synthetic polymers. As such, there are no directly implementable results. However there are some major findings which will lead to implementable results based on the conclusions contained herein. Maleation and chlorination of polymers prior to incorporation into polymer modified asphalt cements provided improved compatiblity. Further exploration could lead to less expensive, easisier to handle modified asphalt cements which would be more stable. Additionally, a constant stress creep test appears to provide an excellent opportunity as a test for compatibility. This test should be developed for use.

TABLE OF CONTENTS

LIST OF TABLES

TABLE OF FIGURES

INTRODUCTION

Asphalt cement (AC) has been the least expensive, most versatile material available for most applications in highway constructions [1]. Asphalts, the residues left after distillation of the more volatile fractions of crude oil, vary significantly from crude to crude, both in their characteristics and in the constituents present. A wide variety of relatively high molecular weight hydrocarbon structures are present in asphalts, but three basic families of compounds are generally recognized to coexist: straight or branched aliphatic chains, simple and complex naphthenic rings, and heteroaromatic systems. Heteroatoms, mainly nitrogen, sulfur and oxygen form the primary functional groups in asphalts along with some complexing metals, such as nickel and vanadium. (Table 1). The functional groups affect the interactions of molecules with each other and with the aggregate [2].

It is impractical to separate and identify all the different molecular species in a given asphalt [3]. Characterization of asphalt generally consists of quantitating generic fractions based on the size and the reactivity and/or polarity of the various molecular types present. In the most generally accepted concept of asphalt composition, asphalts are considered to be composed of asphaltenes and maltenes. Asphaltenes comprising the most complex fraction are mixtures of paraffin elaborated polycyclic structures with molecular weights of 1,000-2,000 daltons); sulfur, oxygen and nitrogen containing heterocycles are also included [4]. This fraction is insoluble when the asphalt is extracted with a nonpolar solvent such as pentane, hexane, or heptane. The soluble component, maltenes, contains both neutral oils and aromatic resins. The resins disperse the asphaltenes in the oils to provide a microscopically homogeneous liquid. [2]. An elution-adsorption chromatography technique [4] can be used to separate a maltene into saturates (n-heptane elutant), naphthene-aromatics (benzene elutant), and polar aromatics (methanol-benzene-trichloroethylene elutant).

It has been long known that asphalts exhibit properties that deviate from those of a true solution and thus may be considered colloidal systems [3], in which micelles are dispersed in a continuous phase of oil. The asphaltene fraction is believed to be associated with the micelle phase. The most nonpolar or saturated fraction is so unlike the asphaltene fraction that the two fractions are not mutually soluble in the absence of

the resinous components (naphthene aromatic and polar aromatic fractions). The coexistence of these phases in asphalt as a microscopically homogeneous mixture is possible because the various components of asphalt interact to form a balanced or compatible system.

TABLE 1

COMPOSITION OF ASPHALT FROM DIFFERENT SOURCES [2]

Source	Mexican	LA/Arkansas	Boscan	California Valley
Code	B-2959	B-3036	B-3051	B-3602
Carbon, %	83.77	85.78	82.90	86.77
Hydrogen, %	9.91	10.19	10.45	10.93
Nitrogen, %	0.28	0.26	0.78	1.10
Sulfur, %	5.25	3.41	5.43	0.99
Oxygen, %	0.77	0.36	0.29	0.20
V, ppm	180	7.0	1380	4
Ni, ppm	22	0.4	109	6

Asphalt compositions are not tightly controlled by manufacturers since they depend strongly on the type of crude oil being processed. At the same time, paving companies use many different aggregates, which call for the use of different asphalt cements. Therefore, rather than try to control asphalt composition, it is better to understand the asphalt one is using and to recognize the interactions between asphalts and aggregates [2]. Models based on asphalt composition have been used by Tuffour et al. [5] and Brule [6]. A Gaestel Index for laboratory aged samples was calculated as [5]:

$$IC=(\%asphaltenes+\%saturates)/(\%naphthene\ aromatics+\%polar\ aromatics) \quad \text{eq. 1}$$

It was found that when IC is correlated with viscosity, susceptibility to aging could be determined from the rate at which the index increases in time. Brule's colloidal instability index is the ratio of the sum of saturated oils and asphaltenes to the sum of

aromatic oils and resins [6]. These models are generally correlated with viscosity - which is a universally accepted indicator of pavement properties, especially for aging studies. However, asphalt composition is difficult to determine and viscosity is not always an accurate measure of compatibility. Most characterization methods for paving grade asphalt cements, including many of those described herein, are empirical in nature. This becomes a problem when modified asphalts are used, because most standard empirical methods were not designed to test them, and serious deviations are often found between test results and actual field performance [7].

The complex mixture of molecules in an asphalt cement means that asphalt has no distinct melting point. It is therefore flexible over a wide temperature range; in pavement asphalt mixtures, the asphalt cement becomes so shear sensitive that the mixture is prone to shove, mar or rut [2, 8, 9]. At low temperatures asphalt becomes glassy and is subject to brittle cracking leading to potholing. Brittle cracking is generally considered to be one of the most significant manifestations of distress in asphalt-surfaced pavements [10]. Cracking is generally reduced by making the asphalt cement either less viscous or less temperature susceptible. Reducing low temperature viscosity leads to soft asphalt and the mechanical properties of the mixture deteriorate. Polymer additives provide more flexibility at low temperatures and higher rigidity under summer heat since these mixes are less temperature susceptible. In fact, the use of asphalt/polymer blends has been progressing rapidly from the experimental stage into mainstream use as the improved physico-mechanical properties of polymer/asphalt cements are demonstrated.

Compatibility of the asphalt binder affects the durability of the asphalt pavement. If the components are not compatible, the highly associated molecular agglomerates in the asphalt become separated from their dispersing or solubilizing components. This makes the asphalt unstable and increases viscosity [5, 11]. The increase in viscosity is also partially due to the loss of volatiles from the binder, which causes shrinkage, leading to residual tensile stresses and cracking [12]. Oxidation causes the formation of carbonyl groups, which also results in hardening, probably due to increased polarity

[13]. Hence, additives may improve properties, but they must be compatible with the asphalt.

POLYMER ADDITIVES

Asphalt has been modified with many different materials, including sulfur, carbon black, lime, metal compounds and polymers. Polymeric materials/asphalt mixtures are complex and characteristically unique paving material systems. For any specific AC/polymer pair, the physical properties of the asphalt-polymer blend are affected by the amount of polymeric material added, its composition, its molecular weight, etc., but the most important variable may be the compatibility of the AC with the admixed polymer. At the same time, developing effective methods to measure the performance of blended asphalt for pavements is a key factor in the acceptance of asphalt cements/polymer products in highway construction.

Polymer additives are not new to asphalt researchers. In Europe, during the past two decades, extensive practical research incorporating several potential polymers into asphalt cements supply preliminary field evaluations; the polymer-asphalt cements provide better, longer-lasting highways. In fact, polymers in Europe have become a permanent part of the roadway construction program [14]. The U.S. paving industry has recently become more interested in so called "polymer modified asphalt." Colorado, for example, has already written polymers into its specifications---all new asphalt surfaces will be constructed with asphalt/polymer blends. There are at least thirty-nine states that have also included polymers to some extent [15, 16].

Polymer additives incorporated into asphalt can be classified into three categories: rubbers, thermoplastics and fibers. Rubbers are non-crystalline polymers with very low glass transition temperatures. The rubber modifies the asphalt to improve especially elasticity and cyclic loading properties of the mixture. Property improvements include: adhesion and tack, durability, softening point and cold flow, impact resistance, resilience and toughness. However, the initial cost of the early rubberized paving products was 40 to 100 percent higher than that of conventional AC paving materials.

Natural and synthetic latexes have been used as asphalt modifiers [17, 18]. Natural latex (poly-1,4-isoprene) has improved chip or aggregate retention and flexibility, increased mixture cohesion or adhesiveness, and reduced temperature susceptibility, resulting in a longer service life. Synthetic latexes used in asphalt include polychloroprene and random poly(styrene-co-butadiene) rubber (SBR). Polychloroprene modified asphalts exhibited increased elasticity, improved cohesion and decreased temperature susceptibility compared to conventional asphalt [18]. SBR modified asphalts had improved flexibility and elastic recovery, better cohesion, a greater resistance to viscous flow under stress, and lower temperature susceptibility than the non-modified asphalt [17, 18]. If SBR is crosslinked after incorporation into asphalt, it may also help prevent aging, since the most reactive sites of the asphalt are consumed during crosslinking and, therefore, cannot be oxidized. Improvements in penetration, viscosity, ductility and tensile stress were registered for AC/SBR mix. A benefit of rubber modified asphalts is that they have the strength of asphalt when unelongated, but the strength of rubber when stretched. Rubber grows stronger due to crystallization when strained, while the asphalt tensile strength decreases [17]. SBS block-copolymers (Kraton or Styrelf) are also elastic but do not necessarily increase the initial stability of the asphalt. However, they are more versatile since the ratio of plastic polystyrene to rubber polybutadiene blocks and the number of arms in a star shaped polymer can be varied at will to influence the final properties of the asphalt mix [17, 19]. The block-copolymers give asphalts improved flexibility, improved resistance to permanent deformation and lower temperature susceptibility and, therefore, extended service life [18, 20, 21].

Plastics give strength to the asphalt, but the ability to recover from extension is lost. [19]. They are useful for asphalt concrete, since it is often designed to be more strong than flexible [18]. Thermoplastics which are partially crystalline such as polyethylene (PE) [22-28], polypropylene (PP) [29, 30] have attracted more and more attention since this class of polymer combines the advantages of rubber and fibers. The crystalline segments of thermoplastics serve as high strength fillers in the asphalt-polymer blend and improve the blend properties over all service conditions. However,

the thermoplastics are much less compatible with asphalt; thus, the blends tend to separate at high temperatures.

Polyethylene, PE, for example, gives asphalt an increased stability and stiffness modulus and increased resistance to permanent deformation . High density linear PE, HDPE, is highly crystalline, melts at about 133°C, and because of the flexibility of the chains has a very low glass transition temperature. The glass transition temperature of asphalts is near 0°C; addition of PE decreases this brittle temperature. This allows PE to contribute additional toughness and ductility at low temperatures to PE/asphalt blends. Linear low density polyethylene, LLDPE (actually a copolymer of ethylene with an α-olefin), increases significantly the viscosity of asphalts when added up to 5%, and therefore reduces temperature susceptibility. This decreases creep and rutting . Addition of 8% LLDPE improves asphalt ultimate strength, flexural modulus, elongation and energy to fracture (area under stress-strain curve) at -20 °C, but low temperature cracking and permanent deformation properties deteriorate in low viscosity asphalt [31]. Using 5-8% PE is feasible, but higher concentrations give mixtures too viscous to be useful.

Since the addition of polyethylenes seems to cause asphalt to fail in a manner similar to that of toughened plastics, one may hypothesize that asphalt toughness is influenced by the particle size of the dispersed phase, the concentration and interfacial adhesion of the additive and the glass transition of the additive, i.e., the fracture toughness of asphalt can be correlated with compatibility [32]. Marshall stability, which empirically measures load carrying capacity, and Marshall flow, a measure of flow to fracture, were shown [32] to increase with the addition of PE (HDPE) to asphalt concrete mix. In addition, polyethylenes with maleic anhydride grafts or small amounts of chlorination were used, since they seem to react favorably with certain components of asphalt, among them carboxyl and free radical groups [33].

Ethylene-vinyl acetate copolymers, EVE, improve resistance to permanent deformation and increase modulus [18, 24]. As a comonomer to ethylene, vinyl acetate decreases the crystallinity of the PE blocks, leading to increased flexibility and toughness. In one study [34] the EVA modified asphalt ranked among the best of the

asphalts tested in the areas of fatigue resistance and field performance. Tables 2 and 3 [16] provide an overview of commercial asphalt polymers and their general characteristics.

The most important parameter governing the success of a polymer modifier in asphalt is its compatibility. As mentioned previously, the asphaltenes are suspended in the oils by the resins, making asphalt a colloidal system. The introduction of any incompatible polymer under agitation into such a system at high temperature generally results in asphaltene flocculation and oil bleeding, leading to a binder having no cohesion [35]. Polymers must improve not only AC properties, but must improve the performance of binder-aggregate combination as well [18]. One compatible polymer may help suspend another. For example, an SBR which did not mix into an inferior AC led to an upgraded asphalt of a very high specification when a small amount of polyolefin was added to the mixture [36].

A polymer is compatible with an asphalt if the modified asphalt exhibits the typical properties of the binders in terms of homogeneity, ductility, cohesion, and adhesiveness [35]. Compatibility can be established if the polymer is soluble in the AC or if it can be swollen by the asphalt oils without causing flocculation of the asphaltenes. An analogy of an elastic sponge filled with a viscous fluid was used [37] to describe the ideal asphalt or modified asphalt. In all cases the asphalt and additive must be compatible and the binder must be compatible with the aggregate.

Other important considerations [17] when using a particular polymeric additive are polymer molecular weight, copolymer composition, chemical modifiers, crosslinked structures, crude source, asphalt compatibility and asphalt viscosity. Age hardening effects are also to be considered since at elevated temperatures some polymer molecules break down, some continue crosslinking, and some separate from asphalt. Aging aspects of polymer/asphalt have not been carefully evaluated.

One of the purposes of our work is to study and to understand significant factors controlling compatibility between asphalt and synthetic polymers. Asphalt-polymer blends with considerably improved physico-mechanical properties, especially higher

TABLE 2

POLYMERS USED IN ASPHALT MODIFICATION

Producer	Type	Trade Name	Dosage/ Total Mix	Mix Time	Mix Temp.	Packaging	Applications	Product Attributes
BASF Corp.	Anionic Latex	Butonal NS-120	3%	n/a	n/a	Bulk/Drums	Chip Seals, Cold Recycling	Improved aggregate retention, flexibility, cohesion
	Cationic Latex	Butonal NS-198	3%	n/a	n/a	Bulk/Drums	Chip Seals, Slurry Seals, Microsurfacing	Improved aggregate retention, flexibility, cohesion
	Cationic Latex	Butonal NS-117	3%	15 min.	160-170°F	Bulk/Drums	Post Addition for Chip Seals	Maintains emulsion viscosity, improved aggregate retention, flexibility
	SBR Latex	Butonal NS-175	3%	5-10 sec. or pre-blended in AC	325°	Bulk/Drums	Hotmix Asphalt, Chip Seals	Minimizes rutting and low temperature cracking, improved aggregate retention and cohesion
	SBR Latex	Butonal NS-134	3%	Pre-blended in AC	n/a	Bulk/Drums	Hotmix Asphalt	Special product for polymer-incompatible asphalts, minimizes rutting and low temperature cracking
E.I. DuPont	Anionic Latex	Neoprene Latex	1-3%	n/a	n/a	Drums	Paving	Wider temperature stability
	Cationic Latex	Neoprene Latex	1-3%	n/a	n/a	Drums	Paving	Wider temperature stability
	Thermoplastic	ELVAX	2%	n/a	n/a	Bags	Paving	Wider temperature stability
	Thermoset	Neoprene	1-3%	n/a	n/a	Bags	Paving	Wider temperature stability
Exxon Chemical Co.	Thermoplastic	Polybilt (wide grade slate allows formulating for different needs/ basestocks)	2.5-5%/AC	varies	varies	50-lb. Bags, 950-lb. Boxes, Pelletized	Hotmix, Chip Seals	Wider temp. stability range, easy low shear blending; Hotmix: Enhanced creep resistance; Chip Seals: Early rock retention
	SBS	Dexco polymer marketed by Exxon Chemical	3-6%/AC	varies	varies	50-lb. Bags, 1000-lb. Box, Other	Surface Treatments, Hotmix	Wider temp. stability range, enhanced low temp. flexibility
LBD Asphalt Products Co.	Thermotropic Polymer	DUCTILAD D1004	3%	Standard	Standard	Liquid, Bulk or 55-gal. Drums	Seal Coat & Hotmix	Improves ductility before and after aging, improves low temp. flexibility
	Liquid Polymer	DUCTILAD D1002	.75-3%	Standard	Standard or lower	Liquid, Bulk or 55-gal. Drums	Seal Coat & Hotmix	Improves ductility before and after aging, improves low temperature flexibility
Rohm and Haas Co.	Acrylic Polymer	Rhoplex AM-2382B	3-20%	<1 hr.	40-350°F	Bulk/Drums	Modify asphalt emulsions	100% Acrylic polymer, excellent ultraviolet resistance
Royston Laboratories *Circle 355*	Polymer	Rosphalt 50	45 lbs.	90 sec.	400°F	22½-lb. Bags	High stability, waterproofing	Increases density, softening point of mix, flexibility at low temps., reduces possible shoving and rutting
Shell Chemical Co.	SBS	KRATON D SBS Rubber	3-9% (Binder Basis)	Same as unmodified AC	320-360°F	50-lb. Bags, 1000-lb. Boxes, Bulk	Surface treatment, Hotmix	Better chip retention, improves rutting resistance, reduces fatigue cracking, improves temp. susceptibility
	SEBS	KRATON G SEBS Rubber	2-6% (Binder Basis)	Same as unmodified AC	320-360°F	50-lb. Bags, 1000-lb. Boxes, Bulk	Surface treatment, Hotmix	Same as above but improved resistance to UV, thermal and oxidative degradation
Textile Rubber & Chemical Co., Ultrapave Div. (Goodyear Tire & Rubber)	Anionic SBR Latex	UP 70	2-5%	Normal	325°F	50-gal. Drums, Bulk	Paving	Lower temp. susceptibility, longer life
	Anionic SBR Latex	UP 70	3%	Co-milled or post-added	260°F or 160°F	same	Surface Treatments, Chip Seals	Improved aggregate retention
	Cationic SBR Latex	UP 65K	3%	Co-milled	260°F	same	Surface treatments, Chip Seals, Slurry Seals, Microsurfacing	same
	Cationic SBR Latex	UP 65K-(VC)	3%	Post-added	160°F	same	Surface Treatments, Chip Seals	same

TABLE 3

GENERAL CHARACTERISTICS OF POLYMER-MODIFIED ASPHALTS [16]

Modifier	Unique Performance	Deficiency	High temp. stiffness	Low temp. flex	Toughness/strength	Low stiffness at processing temp.	Adhesion to aggregate
Styrene/butadiene block copolymer (SBS)	• outstanding toughness • excellent elastic recovery	• mixing/blending • melt storage stability • ductility	+	+ +	+ +	0	0
Styrene/butadiene latex (SBR)	• ductility	• mixing/blending • melt storage	+	+ +	+	-	0
Natural latex	• aggregate retention • good ductility	• mixing/blending • melt storage stability	+	+ +	+	-	0
Polychloroprene (Neoprene)	• toughness • elastic recovery • torsional recovery • compatibility	• ductility • lack of toughness	+	+ +	+ +	-	0
Polyolefin (PE, PP, EVA)	• modulus (stiffness) • aging resistance	• mixing/blending • melt storage stability	+ +	0(+)	0(+)	-	0

rutting resistance important to roads in Louisiana, are expected to be developed. In the present study, a series of chlorinated polyethylenes with different chlorine contents and distributions were synthesized and were mixed with asphalt. Characterization of the asphalt as well as AC-polymer blends is also an important part of our work. Although there are some traditional methods available to determine physico-mechanical properties of asphalt (*vide infra*), they are not sufficient to draw a complete picture of the modified materials. Miscibility and physico-mechanical properties appear more closely related to actual field situations. We have made efforts to employ differential scanning calorimetry (DSC), dynamic mechanic spectrometry (DMS) and thermo-mechanical analysis (TMA) techniques in our studies. Although these techniques are not commonly applied to asphalt characterization, we anticipate that they will provide more information from smaller sample sizes and that the techniques will become part of routine, reproducible analysis procedures for asphalts and asphalt blends.

OBJECTIVES

1. To develop simple analytical methods for determining the compatibility of asphalt-polymer mixtures. An analytical procedure requiring small sample sizes to facilitate a survey of polymer blends was the primary focus of this work.
2. To advance the application of dynamic testing techniques to asphalt evaluation by conducting a baseline survey of selected Louisiana asphalts. The survey includes determination of rheological parameters, glass transitions, low temperature cracking and creep.
3. To evaluate the potential for using differential scanning calorimetry to determine the number of phases and the interaction between the phases in asphalt-polymer blends.
4. To produce a polymer additive from recycled polymers that would enhance the properties of asphalt cement. Successful implementation of the new technology would reduce the burden on the environment of discarded polymers.

SCOPE

After a preliminary evaluation of four Louisiana asphalt samples using the classical techniques of melt viscosity and penetration, a more in depth compositional analysis of eight asphalt samples using NMR and FTIR spectroscopy was conducted. The samples were examined further by differential scanning calorimetry and dynamic mechanical analysis. The results include an assay of the aliphatic and aromatic hydrocarbon contents, the heteroatom or functional group composition, the glass transition, melting point and related thermal transitions, and the rheological properties including creep and low temperature fracture.

Potential utilization of recycled polymers was modeled with high density polyethylene, a common component of polymer waste streams. The HDPE was modified by chlorination because the chemistry of this process can be controlled with respect to the amount and distribution of chlorine introduced. The crystalline polyethylene was converted to a semicrystalline, more polar material by introduction of less than 15 wt% chlorine. The properties of the chlorinated polymers were ascertained.

Using standardized mixing procedures, blends of HDPE and four different CPE samples were prepared and characterized. DSC analysis revealed that all the polymers evaluated produced biphasic blends; epifluorescent microscopy of blends containing 5 and 10 wt% polymer confirmed the presence of a polymer rich phase and a continuous asphalt rich phase. Asphalt blends containing 5 wt% polymer were subjected to dynamic mechanical testing, creep testing and low temperature cracking; the results were compared with the baseline data generated on the standard asphalt samples.

METHODOLOGY

MATERIALS

Characterization of Asphalt Cements The composition of asphalt cements ranges from nonpolar, nonaromatic hydrocarbons to highly aromatic hydrocarbons whose molecular structures contain varying amounts of certain heteroatoms, predominantly oxygen, nitrogen and sulfur. The heteroatoms are often associated with polar, strongly interacting chemical functionality or functional groups which have a disproportionately large effect on asphalt properties. Because the number of molecules in asphalt with different chemical structures and reactivities is extremely large, determination of asphalt composition by separation of asphalt into its molecular components is generally considered impractical. However, the types of functionalities that dominate the properties of the various asphalt types narrows to a manageable number. Many asphalts of different composition may have similar chemical functionalities which in turn produce similar effects on physical properties.

Asphalt is a reactive mixture and its composition may change in time even in the absence of other reactants, such as oxygen. However, the principal cause of age hardening and embrittlement of asphalt in pavements is atmospheric oxidation of certain asphalt molecules to form highly polar and strongly interacting chemical functional groups containing oxygen. Thus, the ability to identify and quantify asphalt chemical functionality provides an important tool for assessing the effects of composition on asphalt properties and, ultimately, the asphalt's performance in service. As part of the present project, a spectral investigation (by Fourier transform infrared, FTIR, and nuclear magnetic resonance, NMR, techniques) of characteristic functional groups present in different kinds of asphalts was conducted. Differential scanning calorimetry (DSC) was employed to estimate crystallinity. Rheological properties of all asphalt samples were studied by dynamic mechanical analysis (DMA). The goal was to achieve an understanding of relaxation mechanisms of asphalt under load at the molecular level. Some asphalt samples were also characterized by standard methods used for asphalt testing.

Physical Testing of Asphalts Temperature susceptibility and shear properties were determined for at least four asphalt cements (AC-10 and AC-20 grades). The viscosity and penetration results were plotted on a bitumen test data chart, and the temperature susceptibility and hardness were obtained from the relation:

$$\text{Log (pen)} = AT + C \qquad \text{eq 2}$$

where A is the temperature susceptibility, T, the temperature, and C, the hardness of the asphalt tested (38, 39). Viscosity evaluation at 60 °C and kinematic viscosity measurements at 135 °C were conducted using a vacuum viscometer and a kinematic viscometer, respectively; the test procedures defined by AASHTO T-202 and AASHTO T-201 were used. The results are summarized in Table 4. Penetration tests (AASHTO T-49) conducted at 25 °C and 10 °C are summarized in Table 5. Calumet AC-10 seems to be the most temperature susceptible and Southland AC-10 the least, as determined from the angle between the penetration and viscosity lines. A larger angle indicates a less susceptible asphalt. The temperature susceptibility, A, was calculated using eq. 2. The angles and the values of A for various combinations tested are reported in Table 6.

NMR and Infrared Spectroscopy The application of NMR to analysis of asphalt samples is well established [40-42]. Samples were dissolved in deuterated chloroform at a concentration of 10% (w/v), and spectra were measured using a Bruker 200 MHz FTNMR. A relaxation agent, $Cr(acac)_3$, 12 mg/mL, was added to the ^{13}CNMR samples. Using an interpulse time of six seconds and more than 8000 scans, reliable quantitative spectra can be obtained [40].

Asphalt samples, 5% (w/v) chloroform solution in 1 mm cell were examined by quantitative FTIR using a Perkin Elmer 1700 FTIR spectrophotometer (Figure 1). The overlapped peaks in 1550 - 1800 cm^{-1}were resolved by a curve fitting program based on the work of J. C. Petersen and his colleagues [41].

Eight asphalt samples with grades ranging from 10 to 30 from four different sources were examined. Table 7 summarizes the observations on our eight samples using the NMR and FTIR techniques. Further, it is known that methine structures,

TABLE 4

VISCOSITY OF TANK ASPHALTS

Asphalt Cement	Sample Code	Vacuum Viscosity @ 60°C AASHTO T-202		Kinetic Viscosity @ 135°C AASHTO T-201	
		No. of Samples	Mean (poise)	No. of Samples	Mean (cSt)
Calumet AC-10	ACA	5	1283.4 ± 113.5	1	330.7
Calumet AC-20	ACB	5	1780.8 ± 35.2	1	395.6
Southland AC-10	ACE	6	1258.3 ± 28.5	2	304.7 ± 2.4
Southland AC-20	ACF	6	2670.6 ± 96.3	2	493.0 ± 3.5

TABLE 5

PENETRATION TESTS ON TANK ASPHALTS

Asphalt Cement	Sample Code	Penetration (25°C) AASHTO T-49		Penetration (10°C) AASHTO T-49	
		No. of Samples	Mean (0.1mm)	No. of Samples	Mean (0.1mm)
Calumet AC-10	ACA	6	118.6 ±2.9	4	25.9 ±1.2
Calumet AC-20	ACB	6	94.0 ±1.2	4	25.3 ±1.2
EXXON AC-10	ACC	4	99.8 ±4.9	4	19.8 ±1.2
EXXON AC-20	ACD	4	66.0 ±1.7	4	11.9 ±0.5
Southland AC-10	ACE	6	151.5 ±1.8	6	41.8 ±1.3
Southland AC-20	ACF	6	84.3 ±1.1	6	18.8 ±1

TABLE 6

TEMPERATURE SUSCEPTIBILITY OF ASPHALT CEMENTS

Asphalt Cement	Sample Code	Angle	A from eq. 2
Calumet AC-10	ACA	142	0.0440
Calumet AC-20	ACB	146	0.0380
Southland AC-10	ACE	147	0.0373
Southland AC-20	ACF	143	0.0434

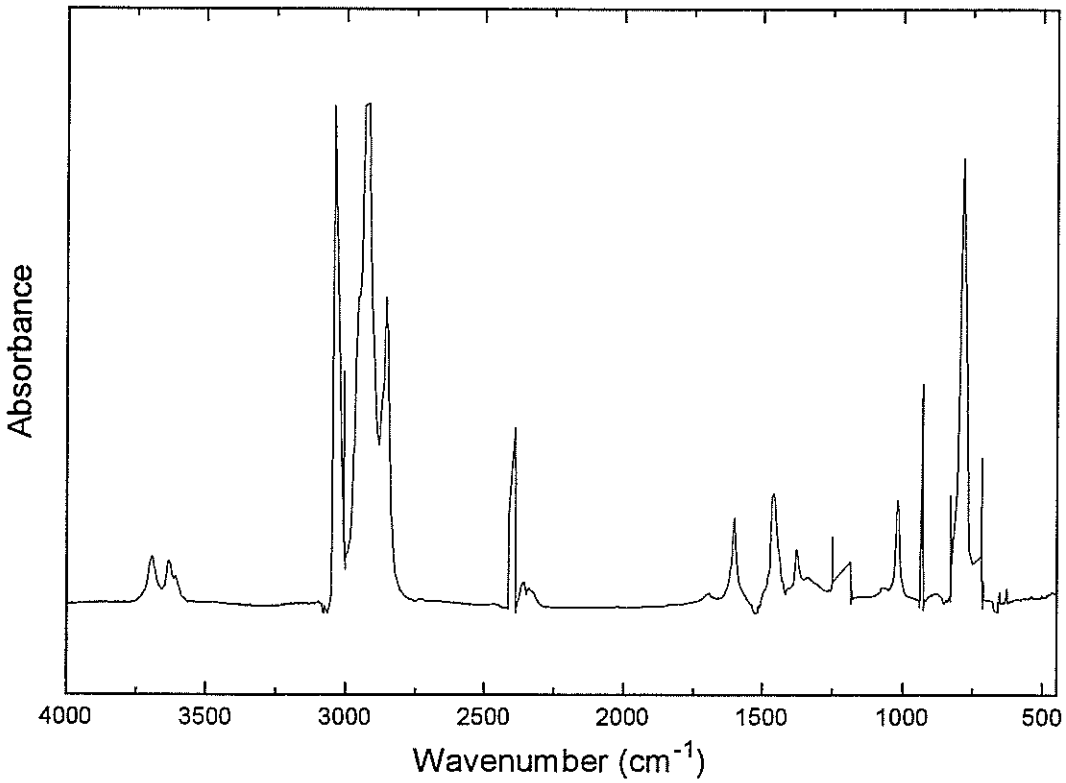

Figure 1. FTIR spectrum of typical asphalt in chloroform.

especially those attached directly to aromatic ring, are the most susceptible sites for oxidation of asphalt, a major cause of pavement failure. We identified the specific aliphatic carbon types in terms of methyl (8), methylene (19) and methine (6) structures with DEPT technique of ^{13}C NMR.

Comparison of DEPT NMR spectra with broad-band NMR spectrum at aromatic band region (100-160 PPM) reveals that no aromatic carbons coupled to hydrogen appear at chemical shifts greater than 131 ppm. The large number of distinctive resonances emphasizes the complexity of the asphalts and suggests that correlating NMR analyses to asphalt chemical and physical properties will be very difficult. FTIR results show significant differences in the composition among asphalt samples of the same grade but from different origins. One must conclude that comparison of asphalt samples based simply on the grade is rather imprecise; an assay of the chemical functionality should be made to more fully characterize the samples.

Differential Scanning Calorimetry. The relative crystallinity of a given asphalt can be measured by DSC [43, 44]. The linear paraffins and alkyl side chains present in asphalt readily crystallize. We used DSC to estimate the relative volume of the crystalline phase in each of the asphalt samples. DSC measurements were carried out using a SEIKO DSC 220C controlled by SSC/5200 data station. The instrument was calibrated for temperature and enthalpy with indium. The DSC was conducted on $\cong$ 10 mg samples sealed in an aluminum sample pan using an empty aluminum sample pan with cap as a reference. Initially each sample was cooled at 3°C/min. to -45°C and then heated at 3°C/min. The heats of fusion (ΔH_f) observed are listed in Table 8. The percent crystallinity was estimated from this data by assuming that completely crystallized hydrocarbons in an asphalt matrix exhibit an average enthalpy of 200 J/g [44].

Polymer/asphalt blends were studied using the same technique. About 10 mg of an asphalt-polymer blend were placed in an aluminum pan and the pan was then sealed and the measurement was made as described above except that the cooling rate was 5°C/min. and the heating rate was 20°C/min. The presence of more compatible polymers is reflected by a reduction in the asphalt crystallinity.

TABLE 7

NMR AND FTIR CHARACTERIZATION OF ASPHALT COMPOSITION

Sample Code	ACA	ACB	ACC	ACD	ACE	ACF	ACG	ACH
Source	Calumet	Calumet	Exxon	Exxon	South-land	South-land	Texaco	Texaco
Grade	AC-10	AC-20	AC-10	AC-20	AC-10	AC-20	AC-20	AC-30
Arom H%	5.5	6.1	6.9	6.0	6.3	6.8	7.1	5.7
Arom C%	28.2	30.4	37.3	34.1	33.4	33.7	34.0	24.5
Linear Aliph%	41.8	41.6	22.5	21.8	19.5	21.2	22.3	23.2
Phenolics*	0.0086	0.0058	0.0069	0.003	0.012	0.0093	0.0036	0.004
Pyrrolics*	0.0142	0.0112	0,0225	0.0135	0.0137	0.014	0.0145	0.0137
Carboxyl Acid*	0.109	0.0828	0.0318	0.021	0.0220	0.0311	0.0242	0.0324
Ketone*	0.133	0.13	0.0275	0.0195	0.0796	0.043	0.027	0.0362
Quinolone*	0.0412	0.0298	0.0269	0.027	0.023	0.0238	0.0175	0.0109
Sulfoxide*	0.0022	0.001	0.0014	0.0036	0.0043	0.004	0.0008	0.0015

* in mmol/g asphalt.

POLYOLEFIN ADDITIVES

Polyethylene (PE) is a potentially useful modifier for increasing the low temperature fracture toughness of asphalt concrete [32], and it may confer additional pavement stability at elevated temperatures, which would minimize rutting and distortion due to creep. If price and availability of various polymers that have been proposed for asphalt modification are considered, it is obvious that polyethylene or waste polyolefins would be more economical than other polymeric candidates. Further, since polyolefins comprise approximately 60% of plastic solid wastes, a reliable source of polyethylene, both as virgin material and as recycled waste is assured. However, it is known that asphalt-polyethylene mixtures have a tendency toward gross phase separation, i.e., gross incompatibility, when standing at elevated temperature for long periods [45]. Therefore, modification of PE is needed to enhance its compatibility with asphalt. Chlorination of polyethylene is a simple technique to change the polarity, to reduce the crystallinity, and to increase the density of the polymer to match the density of asphalt. If the density of the polymeric additive is comparable to that of the asphalt matrix, the driving force for gross phase separation is minimized. Partially chlorinated polyolefin waxes are known to improve stability of asphalt-polymer blends [46, 47], so we elected to prepare and characterize polyethylenes with various degrees of chlorination to improve the polymer interaction with polar components of asphalt.

One of the purposes of our work is to study and to understand significant factors controlling compatibility between asphalt and synthetic polymers. Asphalt-polymer blends with considerably improved physico-mechanical properties, especially a higher rutting resistance that is very important to roads in Louisiana, are expected to be developed. In the present study, a series of chlorinated polyethylenes with different chlorine contents and distributions was synthesized and were mixed with asphalt.

The physical properties of chlorinated polyethylene are dependent on chlorine content and chlorine distribution, which in turn are determined by the technique used for chlorination. Chlorination can be carried out in a homogeneous phase (solution method), or a heterogeneous phase (suspension method). The microstructure and morphology of chlorinated polyethylenes have been studied by several authors [48-53],

and the factors controlling these parameters are documented. In a solution chlorination, chlorine atoms attack the polymer in a random manner; the resultant homogeneous distribution of attached chlorine atoms destroys the ordered arrangement of the polyethylene chain so that the crystallinity of the polymer decreases. Suspension chlorination, on the other hand, leads to blocks of chlorinated ethylene units distributed along the chain, while unchlorinated segments sufficiently long to crystallize remain. In this work, we adjusted the microstructure of chlorinated high density polyethylene by controlling the chlorination temperature. The resulting products were characterized with NMR, FTIR and DSC.

Procedures for Chlorination of Polyethylene High density polyethylene (HDPE) was supplied by Allied Signal Co. The polymer had weight and number average molecular weights of $8.5x10^4$ and $1.9x10^4$, respectively; the melt index was 25. A series of chlorinated polyethylenes (CPE) was prepared either in suspension or in solution. In suspension, the chlorination was carried out at 70, 80, 90 and 100 °C, respectively. In a typical suspension chlorination, 30 g of the HDPE powder was placed in a four-neck reaction flask with 250 mL 1,1,2,2-tetrachloroethane (TCE)(Aldrich Chemical Company Inc. 97%). The vessel was equipped with adapters for a nitrogen inlet and for a chlorine inlet. The suspension was magnetically stirred and placed in a constant temperature bath at 80°C. Under a constant flow of chlorine gas, the reaction was initiated with 2,2-azobis(2-iso-butyronitrile) (AIBN), 0.2g per 1 g of HDPE. After the desired reaction time, the reaction mixture was quenched in a large volume of methanol. The product was separated by filtration, washed several times with methanol and vacuum dried at 55°C for a week.

Solution chlorination was performed in TCE. The polymer was dissolved at 130°C to a concentration of 7 percent (w/v) under nitrogen flow. The solution was then maintained at 110°C with a constant flow of chlorine gas in the presence of AIBN. The system was stirred during the whole process. After the desired time, the reaction mixture was quenched in methanol, washed several times with methanol and vacuum dried at 55°C for a week. The chlorine content was determined with proton NMR. The

chlorine distribution along the polymer chain was analyzed using NMR, FTIR and DSC data. The samples for NMR analysis were run as 15 percent (w/v) solutions in para-dichlorobenzene (Aldrich, spectrophotometric grade). NMR measurements were conducted using an IBM NR/200 FTNMR Spectrometer at 115°C to insure that the entire sample was dissolved. Samples for infrared analysis were prepared by casting a solution of the polymer in TCE on a KBr plate, then the KBr plate was vacuum dried at 55°C for a week. A Perkin Elmer FTIR Spectrometer 1760X was used to perform the infrared measurements. The properties of the CPE's prepared in this study are summarized in Table 8.

Figure 2 shows the FTIR spectra of the high density polyethylene and several chlorinated polyethylenes produced from it. Chlorination conditions with the exception of reaction temperatures were held constant; the temperatures and the resultant chlorine contents are cited in the figure. The strong CH_2 rocking mode of polyethylene with a characteristic splitting due to crystalline and amorphous configurations is observed in the 720-730 cm^{-1} region of FTIR spectrum of HDPE. The peak at 720 cm^{-1} has contributions from methylene sequences in both the crystalline and amorphous phase [49], while the 730 cm^{-1} band is assigned to the crystalline phase alone.

TABLE 8
METHOD OF PREPARATION AND CHARACTERIZATION OF CHLORINATED POLYETHYLENE (CPE).

CODE	Cl%(Wt)	Preparation Method	Heat of fusion (J/g)	Melting Peak (°C)
HDPE	0		343	131
CPEA	2.7	solution	301	125
CPEB	8.9	solution	206	114
CPEC	15.2	solution	99	106
CPED	21.8	solution	-	-
CPEE	6.5	suspension	215*	130*
CPEF	16.2	suspension	209*	128*
CPEG	36.1	commercial	-	-

* The heating rate was 20°C/min.

The method of chlorination has a major effect on both band intensity and band splitting. Comparison of the spectra of polymer with similar chlorine contents shows that the bands are weaker for CPE prepared at 100°C with 14% chlorine (spectrum D) than those for CPE prepared at 80°C with 16% chlorine (spectrum C), and, in spectrum E, the 730 cm^{-1} band becomes a shoulder. The changes in these bands are caused by decreasing crystallinity as the number of unchlorinated methylene segments long enough to crystallize decreases. The density and clear splitting of these bands suggest that the CPE's prepared at 70 or 80°C are blocky, while those prepared at 100°C or in solution have random distribution.

The C-Cl stretching bands at 615 and 660 cm^{-1} are assigned to isolated chlorine atoms in the TT and TG conformations, respectively [54]. A band at about 685 cm^{-1} has been identified with vicinal chloride structures, such as, -CHCl-CHCl-, or -CHCl-CHCl-CHCl-. As can be seen in spectra D and E, there are clearly two peaks at 660 and 615 cm^{-1}. However, the 660 cm^{-1} band is broadened and shifted toward higher wave numbers in B and C, which may be indicative of the presence of vicinal chlorides that contribute to a peak at 685 cm^{-1}.

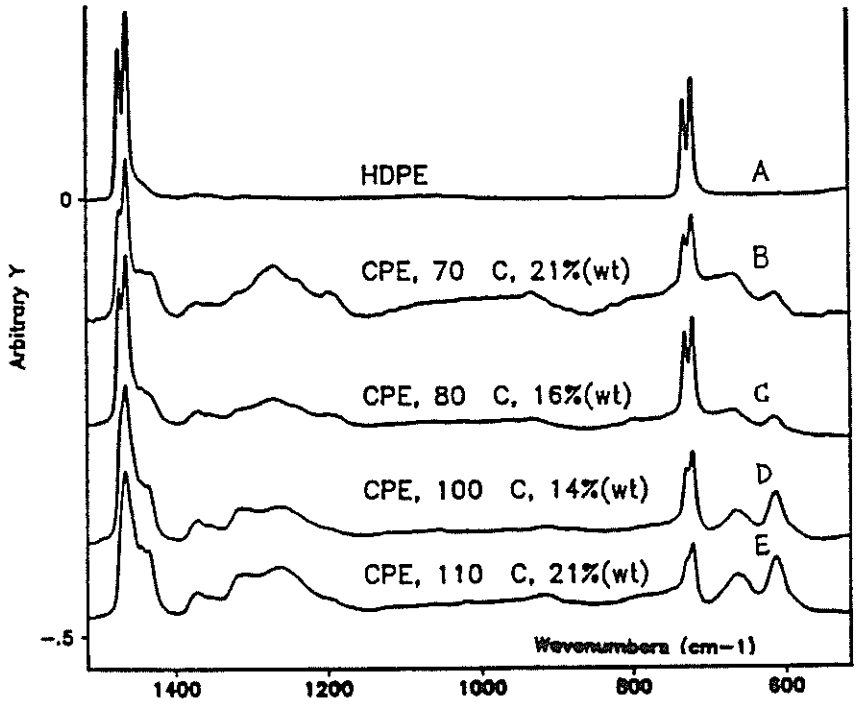

Figure 2. FTIR spectra of chlorinated polyethylenes

DSC Characterization of CPE Samples A DSC thermogram of CPE containing 19 wt% chlorine prepared heterogeneously at 90°C consists of a single endotherm centering at 127.5°C; the heat of fusion, (ΔH_f), is 134.4 millijoule per milligram of sample. The corresponding ΔH_f of pure polyethylene is 200 mJ/mg so it is apparent that chlorination converts crystalline HDPE into a more amorphous material. The heat of fusion can be converted from millijoule per milligram CPE into joule per gram CH_2 units, called reduced heat of fusion, to make it more sensitive in describing chlorine distribution along the polymer chains. Figure 3 is a plot of the reduced heat of fusion versus chlorine content for CPE's prepared under different conditions. A significant influence of chlorination method and temperature can be observed on the reduced fusion heat of samples with similar chlorine content. In suspension chlorination, the initial attack of chlorine occurs in the amorphous regions including adjacent crystalline

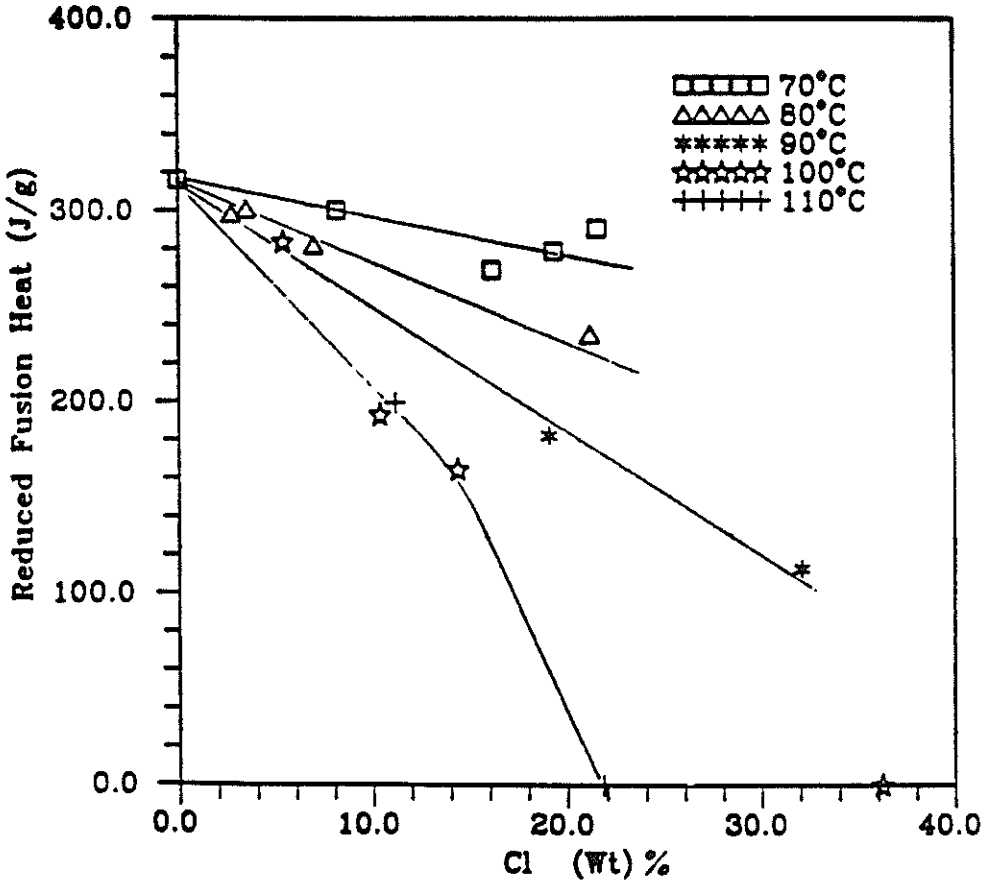

Figure 3. Reduced heat of fusion of CPE's with various chlorine contents prepared at different reaction temperatures

surfaces [55-57]. Further chlorination can occur by penetration of chlorine through the chlorinated surfaces with attack on the densely packed chains in the crystal. Thus, the crystallinity can be selectively decreased by either introducing high chlorine contents or by increasing the randomness of the chlorine distribution.

The DSC results show that, in the temperature range of this study, elevating the reaction temperature will increase randomness of chlorine distribution on chlorinated high density polyethylenes. A premelting transition observed in HDPE allows more random chlorine substitution if the suspension chlorination is conducted at 100 °C or above. Proper temperature control can enable one to adjust both microstructure and morphology of CPE while introducing less than 20 wt% chlorine. The CPE samples retain sufficient crystallinity to serve as fillers in an asphalt/CPE blend.

Asphalt/Polymer Blends, APB Mixing techniques for preparing asphalt polymer blends have been described in several patents (21, 33, 58, 59). In some cases as much as 10% polymer was claimed in the mixture, while in others no more than 3% polymer was mixed. When higher concentrations of polymers were used, it is very likely that the oils that usually peptize the asphaltenes were adsorbed by polymeric material. If the polymer phase removes a large fraction of the oil component, the asphaltene may flocculate, substantially diminishing the useful properties of the asphalt cement [33]. Therefore a concentration of 5% by weight of polymer in the AC/polymer mix was used unless otherwise specified (see figs. 10-17).

Results from preliminary mixing experiments suggest that the best asphalt polymer blends are produced when the mixing temperature is above the melting point of the polymer crystallites. Therefore, the asphalt polymer blends were prepared by melting the desired quantity of polymer in AC-10 at 150 °C while stirring at a rate of 200-500 RPM for two hours under N_2 atmosphere. In one example, one percent maleic anhydride (MAH) was added into the blend containing five percent CPED to enhance the compatibility of the mix. The polymer phase recrystallized upon cooling to room temperature.

DMA Bending Mode Measurements In a typical DMA experiment, an asphalt sample was heated to 150 °C in a sand bath. The asphalt sample was then poured into a brass mold and kept at room temperature for at least an hour. Molded asphalt bars, 20 x 9.495 x 1.64 mm (l x w x t) were mounted in a Seiko DMS 110; each sample was run in bending mode at cooling rate of 1°C/min. at a single frequency. Operating at a single frequency over each temperature range yields more reproducible data that attempting to obtain multifrequency data in a single run. Since multiple runs are required establishing the relationship between frequency and temperature, this approach is very time consuming but we believe that it is necessary. The T_g was identified as the temperature corresponding to the maxima of the loss modulus, E", at each frequency. If the T_g is plotted against corresponding frequency based on an Arrhenius equation, an activation energy for the relaxation process can be computed. Table 4 (page 14) summarizes T_g's and the calculated activation energies, E_a, for our asphalt samples.

Imposition of a larger strain (1%) on the asphalt samples at 50 Hz in DMA experiments will induce cracking at a specific temperature during the cooling. The temperature, called cracking temperature (T_c), can be used to estimate the low temperature cracking resistance of asphalt or asphalt/polymer blends.

DMA Shearing Mode Measurements The shearing mode measurements were conducted at temperatures well above the glass transition temperature of asphalts and polymers employed. A SEIKO DMS 110 in shear mode (parallel plate mode) controlled by SDM5600 Rheostation was used in this study. The sample was applied to the plates with cross section of 10x10 mm. The thickness of the sample was first approximately adjusted and then the sample was held at 45°C for thirty minutes to allow it to relax completely. After the sample was cooled to room temperature, the final thickness was measured with an error of $\pm$0.01 mm. Sample thickness was held to about 1.5 mm, measured with a deviation of $\pm$0.05 mm. The strain was held to less than one percent to ensure linear viscoelasticity. Master curves were calculated using a reference frequency of 20 Hz.

Thermal-Mechanical Analysis, TMA A constant load was imposed on a sample for 10 minutes, then the load was lifted and the sample was kept in free state for another 10 minutes. The strain response was measured as a function of time (Figure 4). The sample geometry and loading mode for the TMA tests are shown in Figure 5. The load was one gram in shear mode and the sample area is about 15 mm^2, which was measured individually. The test temperature was 25.6 °C.

Constant Stress Creep Test The test was run at 5, 15, 25, 35 °C, respectively, with Bohlin CS rheometer using a cone and plate mode. The stress applied was 590 Pa.

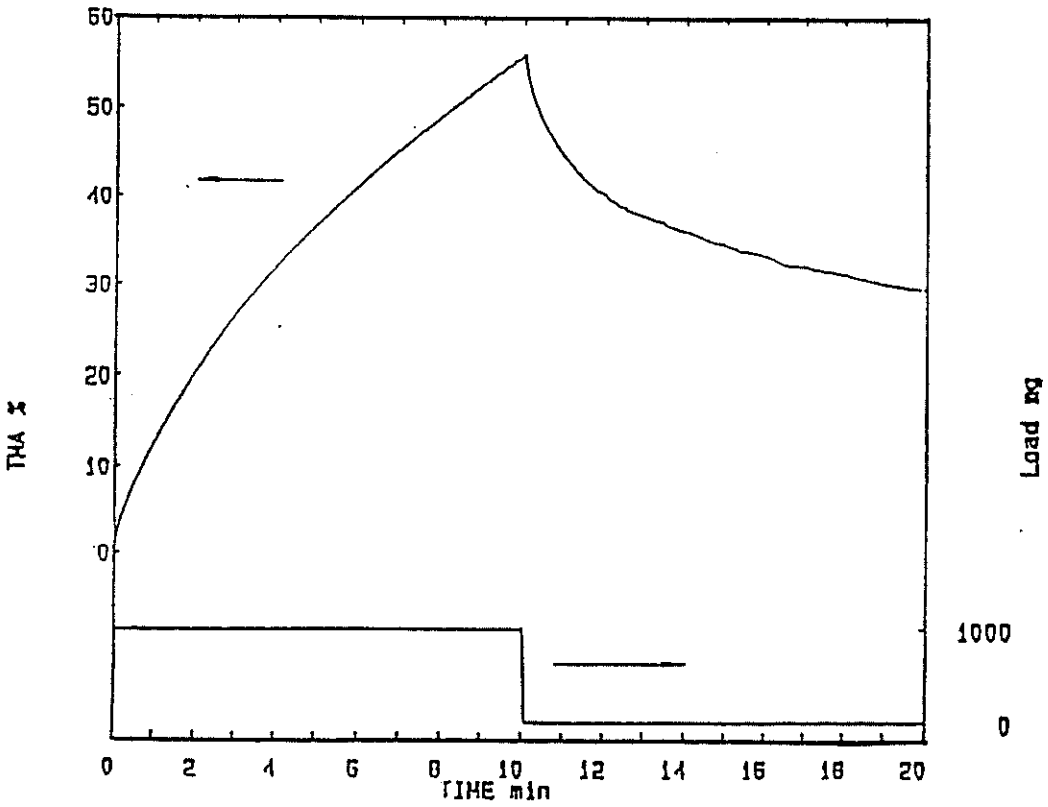

Figure 4. Typical TMA creep test.

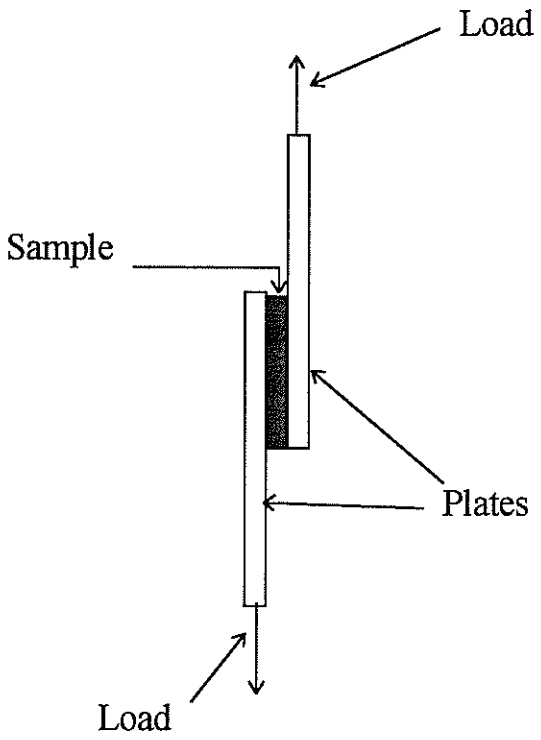

Figure 5. Sample geometry and load mode for TMA creep test.

RESULTS

PHYSICAL TESTING OF ASPHALT/POLYMER BLENDS

Characterization of asphalt/polymer blends has been limited to correlations between macroscopic properties and specifications or performances of a material. Correlating the macroscopic properties and performances exhibited by a material has not been successful because many standard physical tests have failed to predict field performance effectively [2, 60]. Understanding microscopic behavior of asphalt components and their interaction with polymer additives may be a more applicable to predicting field performance, thus we are interested in microscopic behavior of our systems.

Blend compatibility is one of the most critical physical properties of asphalt-polymer cements. Poor miscibility will undoubtedly cause the system to fail as phase separation occurs, however, a completely miscible system may not possess the desired properties to reinforce the composite. A successful product should be a three dimensional co-continuous network structure even at a low concentration of the minor phase[61]. Due to the complexity of components present in asphalts, the addition of polymer is expected not only to be related to compatibility of asphalt and polymer but also to affect the dispersion of individual component of asphalts. We have attempted to assess blend compatibility using DSC. The macrostructure of the asphalt polymer mixtures was examined using fluorescence reflection microscopy (FRM).

Compatibility Analysis by Differential Scanning Calorimetry DSC uses a method of heat flow measurement based on either heat flux or power compensation [62]. The DSC technique is commonly used in material research to measure (i) glass transition temperatures (T_g) (or secondary transition temperatures (T_r)), (ii) melting points (T_m), (iii) heats of fusion (ΔH), etc. Figure 6 is an example of DSC thermogram, complete with DDSC (derivative DSC), a useful technique to identify secondary transition temperatures. The DDSC is the upper curve in the figure. DSC has the advantages of small sample requirements, relatively rapid measurement capability, high sensitivity (ability to detect dispersion phases with a size as small as 10^{-3} mm [61])

and the ability to make measurements over a very wide temperature range (-150°C to 550°C for the instrument used in this study). Information about morphology, miscibility and thermal behavior of asphalts and asphalt-polymer blends can be obtained through analyzing their DSC thermogram.

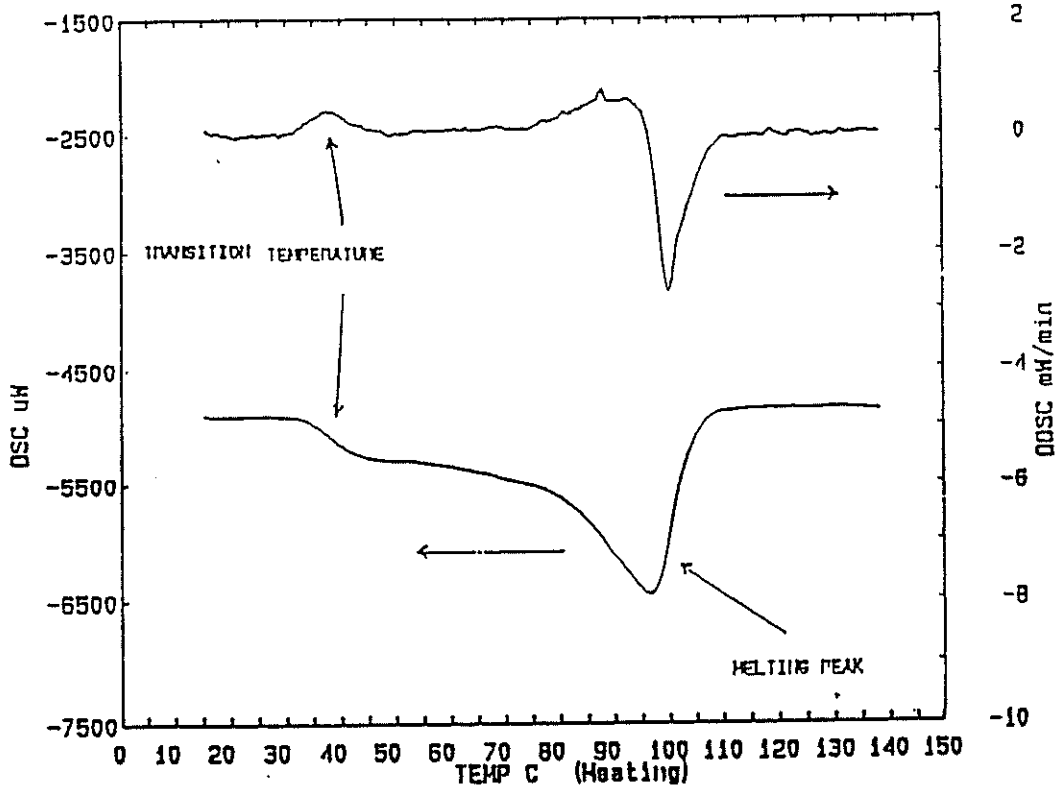

Figure 6. An example of a DSC thermogram.

The thermal behavior of asphalts is complex and depends on their sources, methods by which they are manufactured, and thermal history. For example, the DSC curve of ACE shown in Figure 7 indicates that there are three transition temperatures (T_r) at -42°C, -10°C and 43°C and one melting peak at 28°C. In order to facilitate discussion, these transition temperatures and their correspondence in ACE/polymer blends to be mentioned below are identified as T_{r1}, T_{r2} and T_{r3}, respectively. Figure 8 shows a DSC thermogram of CPEC, a chlorinated polyethylene containing 15.2%

chlorine, which will be blended with the asphalt. Two transition temperatures at -15 °C and 80 °C and one melting peak at 106 °C can be detected.

A thermogram of a blend of CPEC with ACE (20/80, w/w) (Figure 9) reveals that: (i) there is a T_r at -43°C that is the same as T_{r1} in ACE, (ii) a new T_r is observed at -13 °C instead of T_{r2}'s at -10°C and -15°C for ACE and CPEC respectively, (iii) the melting peak for ACE and the 80°C T_r for CPEC disappears, leaving an intermediate T_r of 42° C, (iv) the melting peak for CPEC at 106°C lowered to 95°C. Figure 10 shows the DSC curves of ACE/CPEC blends of various concentrations. T_{r1} was unchanged and T_{r2} varied slightly. The melting peak of ACE cannot be seen in all blends, but the T_{r3} transition becomes stronger when polymer concentration increases. The melting peak of CPEC was shifted downward a maximum of 12°C at a CPEC concentration of 10 wt%. The corresponding thermograms for ACE blends with CPEA (2.9 wt% Cl) and CPEB (8.9 wt% Cl) are shown in Figures 11 and 12, and 13 and 14, respectively.

Figures 15 and 16 are thermograms of ACE/HDPE blends at various concentrations. Note that T_{r1} broadens as the concentration of HDPE is increased and T_{r2} disappears at 30 percent HDPE, and the melting peak of ACE disappears in all blends. The HDPE melting peak is shifted a maximum of 12°C at 10% HDPE and then shifts upward as the HDPE concentration increases (Figure 16).

The multiple transitions observed in the DSC thermogram of ACE (Figure 7) shows that ACE, as most asphalts, is a heterogeneous rather than a homogeneous system. It has been found that saturates and aromatics make the main contributions to thermal effects observed in DSC thermogram of asphalts [44]. After the asphaltenes were removed from ACE by solvent extraction, all three of the transition temperatures decreased, and no crystalline fraction was detected. The transitions of ACE become broad or weak as the concentration of HDPE increases, and no asphalt melting point is observed. Clearly, HDPE interacts with the saturates fraction and extracts them from the asphalt. In contrast, the transitions of ACE become stronger when the concentration of CPEC increases; blends of CPEA and CPEB exhibit intermediate

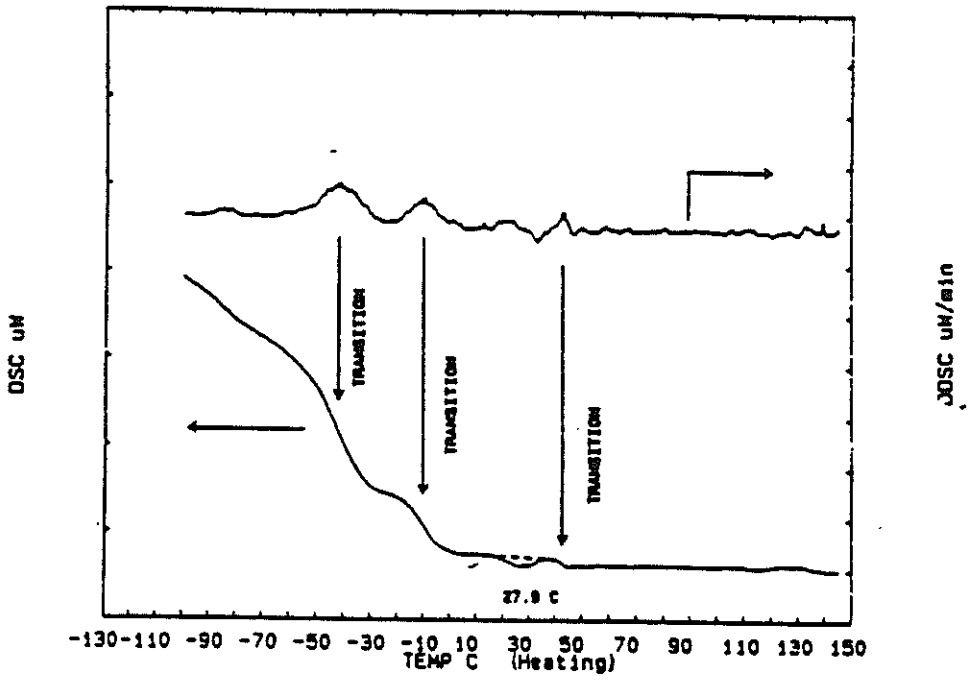

Figure 7. DSC thermogram of an AC-10 asphalt, ACE.

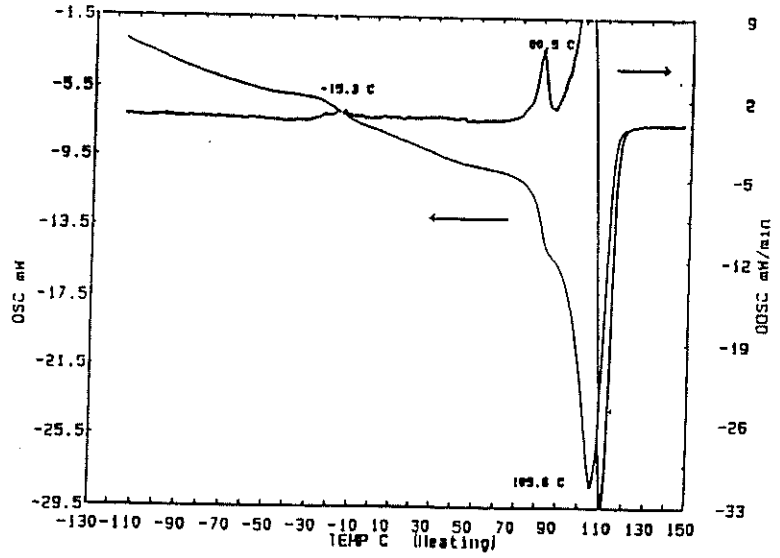

Figure 8. DSC thermogram of a chlorinated polyethylene, CPE.

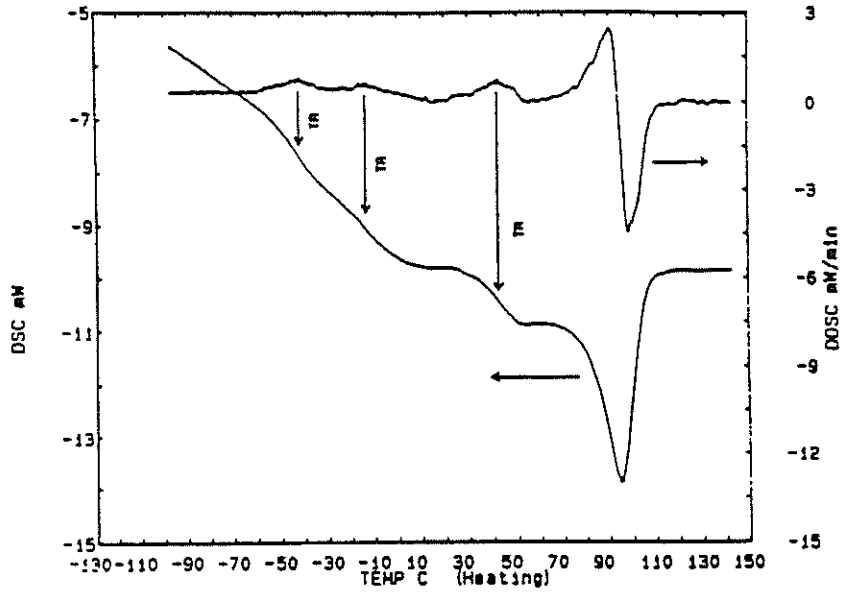

Figure 9. DSC thermogram of a blend of ACE with CPEC, (80/20)

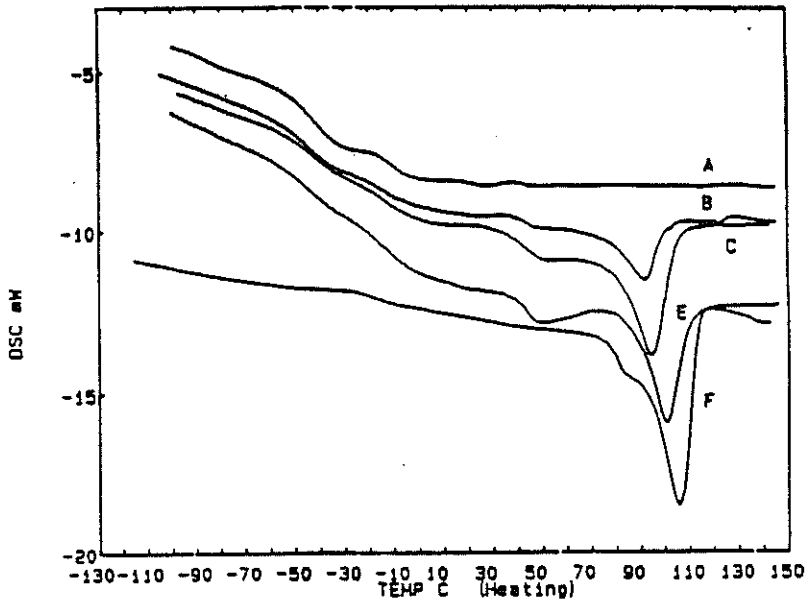

Figure 10. DSC thermogram of blends of ACE with CPEC at varied weight ratios: A, 100/0; B, 91/10; C, 80/20; E, 70/30; F, 0/100.

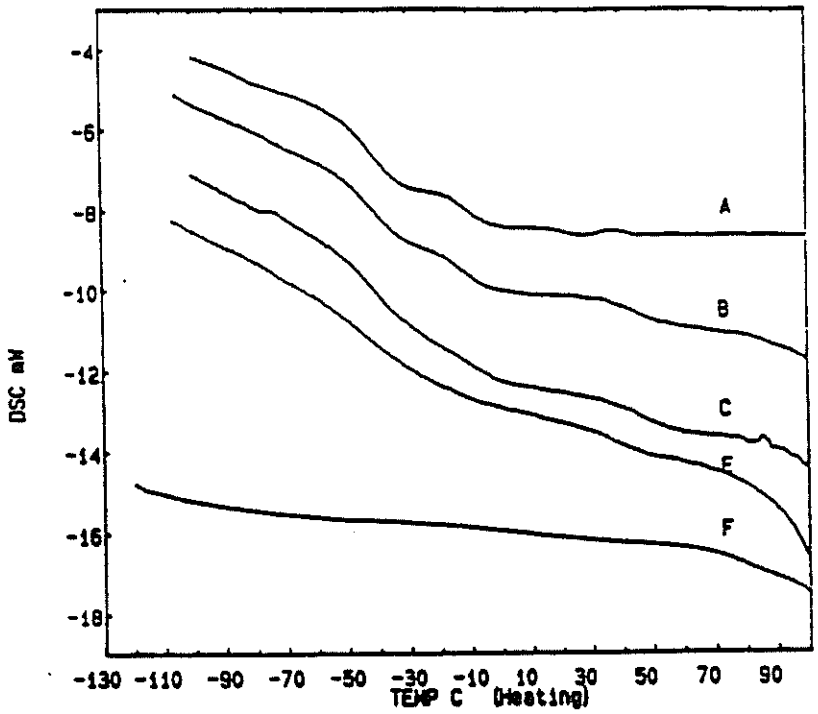

Figure 11. DSC thermogram of blends of ACE with CPEA at varied weight ratios: A, 100/0; B, 91/10; C, 80/20; E, 70/30; F, 0/100

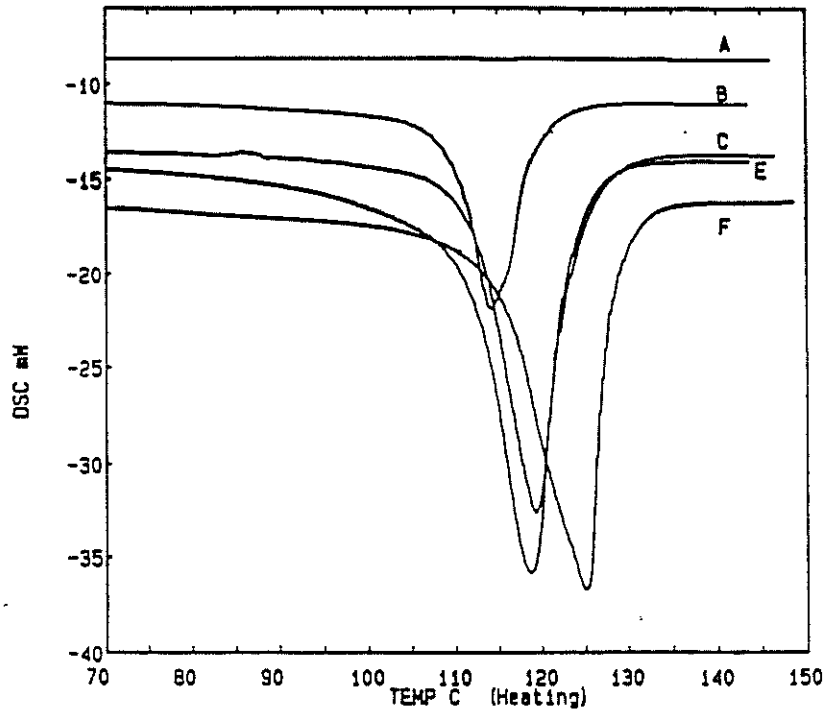

Figure 12. DSC thermogram of blends of ACE with CPEA at varied weight ratios: A, 100/0; B, 91/10; C, 80/20; E, 70/30; F, 0/100

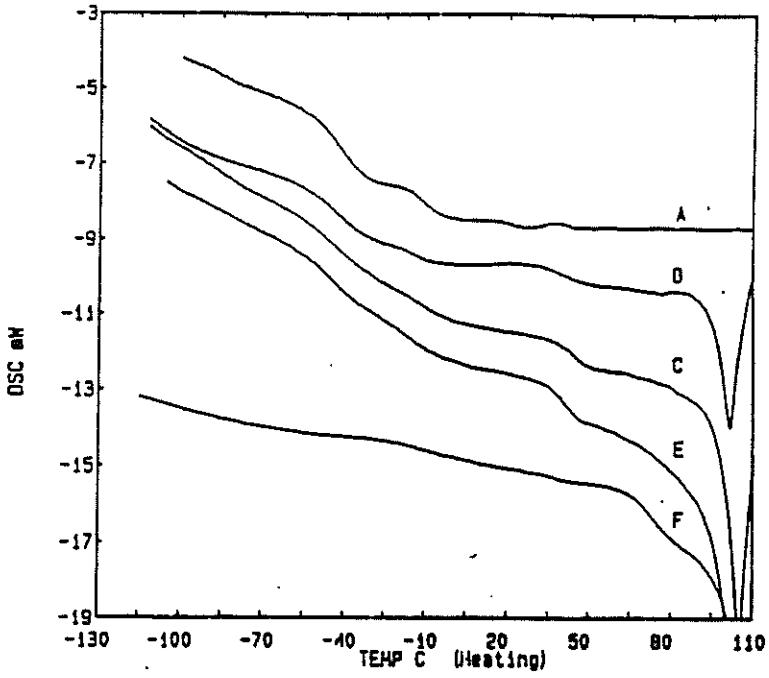

Figure 13. DSC thermogram of blends of ACE with CPEB at varied weight ratios: A, 100/0; B, 91/10; C, 80/20; E, 70/30; F, 0/100

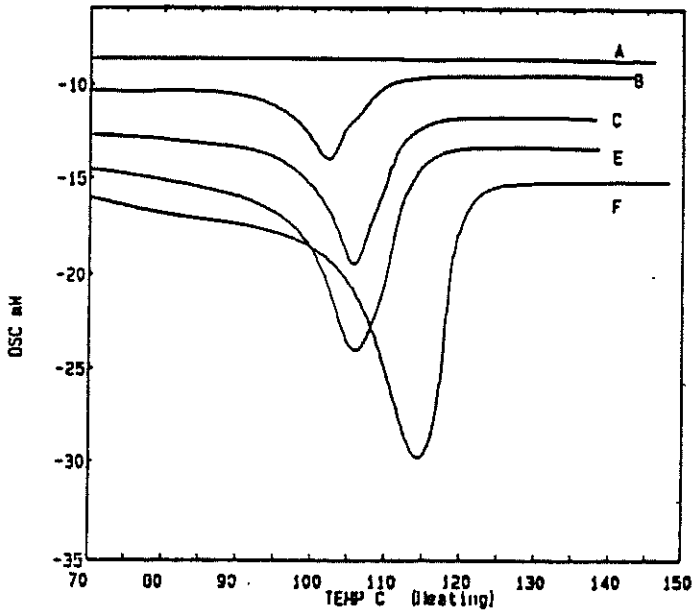

Figure 14. DSC thermogram of blends of ACE with CPEB at varied weight ratios: A, 100/0; B, 91/10; C, 80/20; E, 70/30; F, 0/100

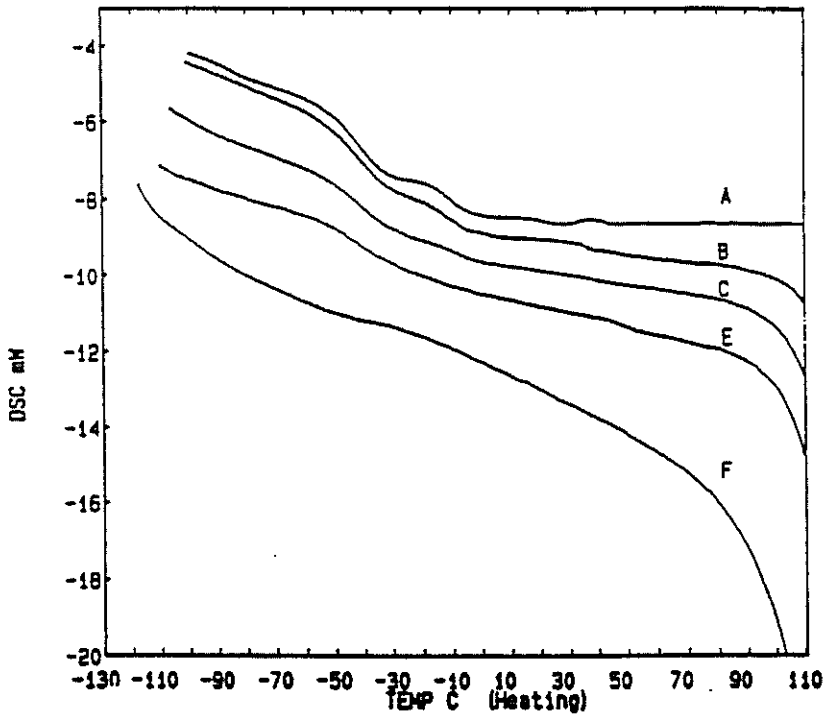

Figure 15. DSC thermogram of blends of ACE with HDPE at varied weight ratios: A, 100/0; B, 91/10; C, 80/20; E, 70/30; F, 0/100

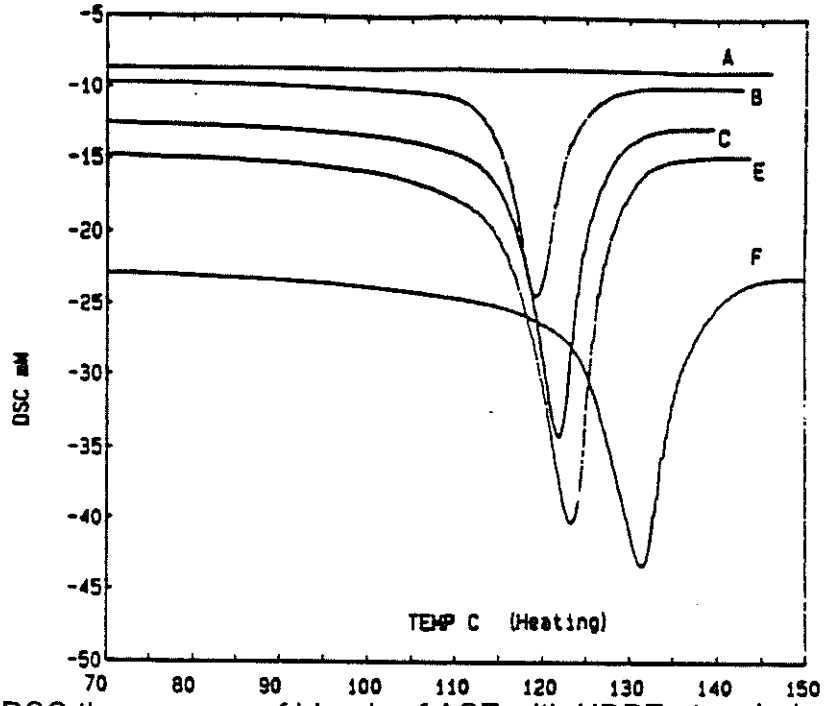

Figure 16. DSC thermogram of blends of ACE with HDPE at varied weight ratios: A, 100/0; B, 91/10; C, 80/20; E, 70/30; F, 0/100

properties. Apparently, introduction of chlorine atoms onto the polymer chain adjusts the interaction parameters to reduce single component extraction, which will make it possible to keep the delicate equilibrium among components of asphalt.

All melting peaks from polymers moved toward to lower temperatures as the polymer concentration decreases. The melting point depression indicates that there are interactions between the polymers and ACE and the magnitude of the shift indicates the extent of the interactions. If polymer and asphalt are miscible to any extent, crystals of the polymer will be in equilibrium with a mixed amorphous phase. The melting point will be lower than when the equilibrium is with a pure amorphous phase of the same component comprising the crystals [63]. The component in equilibrium with polymer crystallites is probably derived from the saturates of ACE, since the crystallites are also composed of hydrocarbon chains. There are sufficient quantities of saturates in ACE to plasticize low concentrations of polymer; however as the concentration of polymer is increased beyond 10%, the saturates are completely extracted and the relative concentration of the plasticizer decreases. Thus, the reduction in the melting point depression as the polymer concentration increases confirms the complete extraction of asphalt components into the polymer phase. These results suggest that high concentrations of any polymer additive will disrupt the compatibility of the asphalt mixture.

The heat of fusion from DSC data for ACE/HDPE indicates that most of HDPE crystallinity remains intact in the blend. The melting point depression, on the other hand, reveals that part of the saturated aliphatic oil was extracted from the asphalt phase into the HDPE phase. Since the saturated component usually represents only a small part in asphalt, the HDPE phase may be just slightly swollen. A brief morphologic description of ACE/HDPE blend, therefore, will be that the swollen HDPE particles disperse among the continuous asphalt phase. Epifluorescence microscopy provides a confirmation of this hypothesis.

Characterization of Polymer Dispersion by Epifluorescence Microscopy It has been reported [35,64] that asphalt polymer blends prepared by physical mixing of constituents are generally two phase systems, which can be observed with optical or

electron microscopy. In many cases, the phase dimension in polymer modified asphalt is large enough to be observed under an optical microscope. Reflection optical microscopy allows the observation of the material in the intact state. However, it provides only a very superficial view of the phase structure. By far the most valuable method is fluorescent microscopy, where the blend is illuminated with an exciting ultraviolet light. The polymer phase or polymer enriched phase re-emits a yellow light whereas the asphalt phase does not give rise to observable fluorescence [65]. Figure 17 shows the epifluorescence microscopy images of HDPE/ACE blends and CPEC/ACE blends, respectively, which confirm previous reports that there are basically two phases existent in asphalt-polymer blends, an continuous asphalt rich phase and a polymer rich phase. The dispersed polymer rich phases are expected to improve the toughness of brittle asphalt at low temperature and reinforce asphalt at high temperatures [66, 67]. The CPE rich phase is larger than the HDPE rich phase in asphalt blends prepared under comparable conditions, indicating that a higher percentage of the asphalt components have been absorbed in the polymer phase. Samples containing 10 wt% CPEC exhibit bicontinuous phase morphology; the phase transformation is accompanied by a marked increase in viscosity. Blends with 10 wt% HDPE retain the polymer droplets in an asphalt continuous phase.

The enhanced compatibility of CPE in asphalt can be attributed to a change in the polymer polarity as well as changes in morphology stemming from the reduced crystallinity. In crystalline polymers like HDPE, interaction with solvents and reagents is limited to the readily accessible amorphous regions. In HDPE, these regions are composed of $-CH_2-$ segments more compatible with the saturates in asphalt. One would expect selective extraction of the saturates from the asphalt matrix by HDPE; this process would disrupt the balance of components in asphalt mixtures and promote phase separation. Although chlorination of HDPE was conducted in solution, analysis of the chlorine distribution in the chains indicates that chlorination is not perfectly random. Runs of unreacted methylene groups that can crystallize remain. Chlorinated methylene groups do not enter the crystallites so the amorphous region contains a

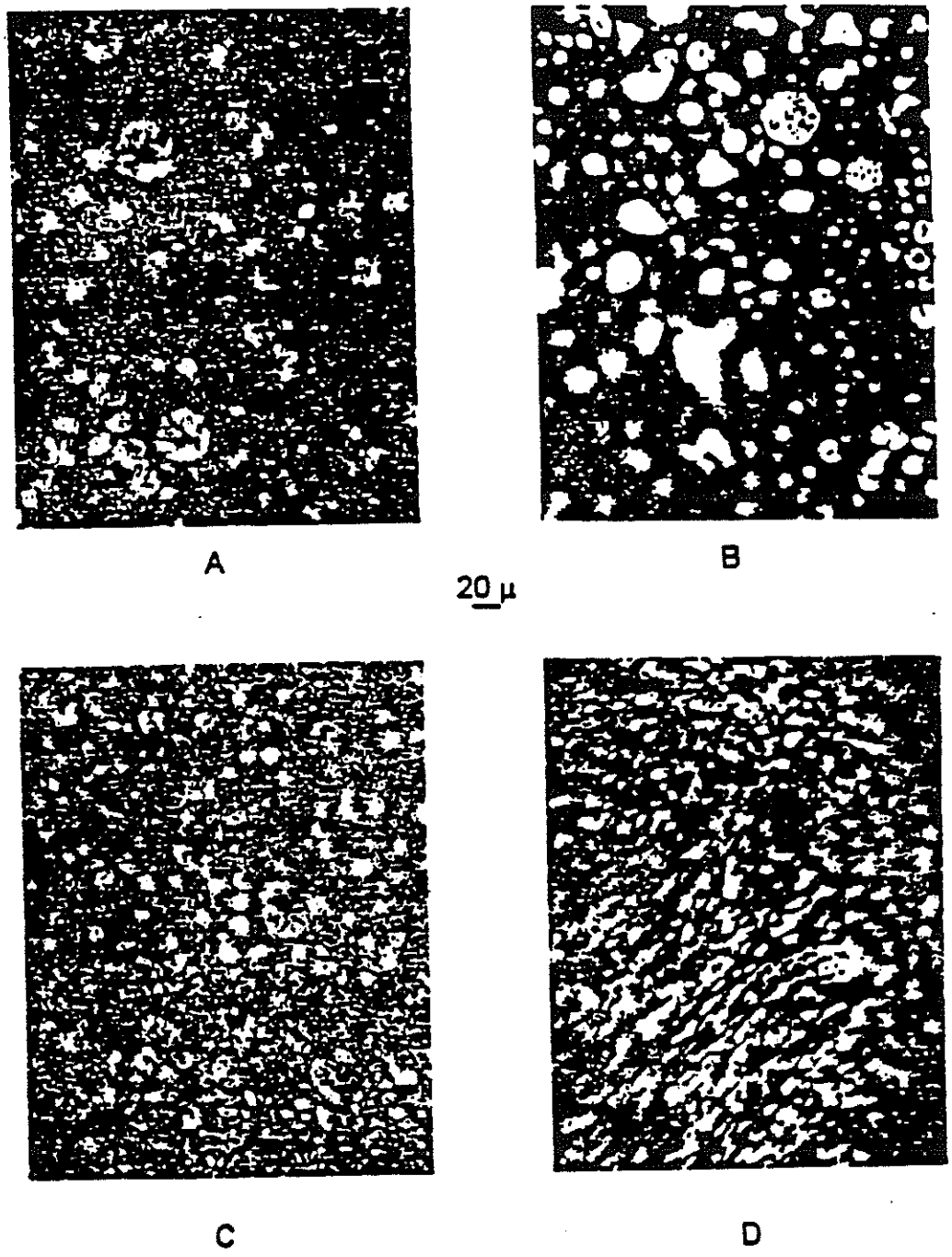

Figure 17. Epifluorescent microscopy images of asphalt/polymer blends: A, ACE-5% HDPE; B, ACE-5% CPEC; C, ACE-10% HDPE; D, ACE-10% CPEC

higher chlorine content than that measured in bulk samples. Thus, the amorphous regions are substantially more polar, and the presence of chlorine atoms on the polyolefin chain will improve the compatibility of the polymer with asphalt components and functional groups containing heteroatoms, such as, N, S, and O. The polar components of asphalt would have a greater affinity for the amorphous regions of CPE and one would expect a corresponding increase in the compatibility of these polymers with asphalt. Introduction of chlorine adjusts the interaction parameters to reduce single component extraction thus the delicate equilibrium among the asphalt components is maintained.

Thermal Mechanical Analysis(TMA) TMA is a technique in which the deformation of a substance is measured under non-oscillatory load as a function of temperature as the substance is subjected to a controlled temperature program [62]. TMA is very effective in conducting tests like creep, stress relaxation and stress-strain with good temperature control over a wide temperature range, but has some stringent sample preparation requirements. We performed creep tests with this equipment in a effort to access the rutting resistance of the asphalt/polymer blends. However, the limited loading and extension ranges of the equipment forced us to work at room temperature. Figure 18 shows that the polymer additives increase the creep resistance of AC-10. The sample elongations attained at 10 minutes are the same for all the ACE polymer blends. However, there are considerable differences in the shape of the curves. Elongation vs. time plots for blends containing highly crystalline polymers are straight lines (B, C), and the plot for the CPEB (less crystalline polymer) blend is only slightly curved. Blends containing amorphous or rubbery polymers exhibit less linear elongation vs. time relationships. The differences may be due to the differences in phase distributions discussed above, but the restricted measuring conditions imposed by the TMA equipment prevented further examination of samples.

A long term creep test was conducted with a homemade apparatus which applied static stress. The load was 22.4 gram in tensile mode, the sample cross section was 1.0 x 0.6 cm^2 and the testing temperature was 23.5 $^{\circ}C$. The data in the resulting plot (Figure 19) indicate that there is a significant improvement in the creep resistance of polymer

blends compared to AC-10. The pure asphalt sample failed within two minutes under the testing conditions. A HDPE blend was more creep resistant but it exhibited a brittle failure after 45 minutes. Heterogeneously chlorinated CPE (6.5 wt% Cl) was more resistant to elongation, but it also failed at 75 minutes. Homogeneously chlorinated CPE samples (21.4 wt%) were quite ductile as might be expected because these samples are not crystalline.

A standard ductility test, AASHTO T-51, was conducted in a 4 °C water bath with 5 cm/min. pulling rate. Figure 20 shows that ACE has a low modulus and large elongation. Crystalline HDPE and CPEE containing blends exhibit moduli and low elongations terminating with brittle failure. Amorphous CPED containing blends exhibit moderate moduli and high elongation; the increase in stress required at higher elongations are consistent with the behavior of a rubbery material.

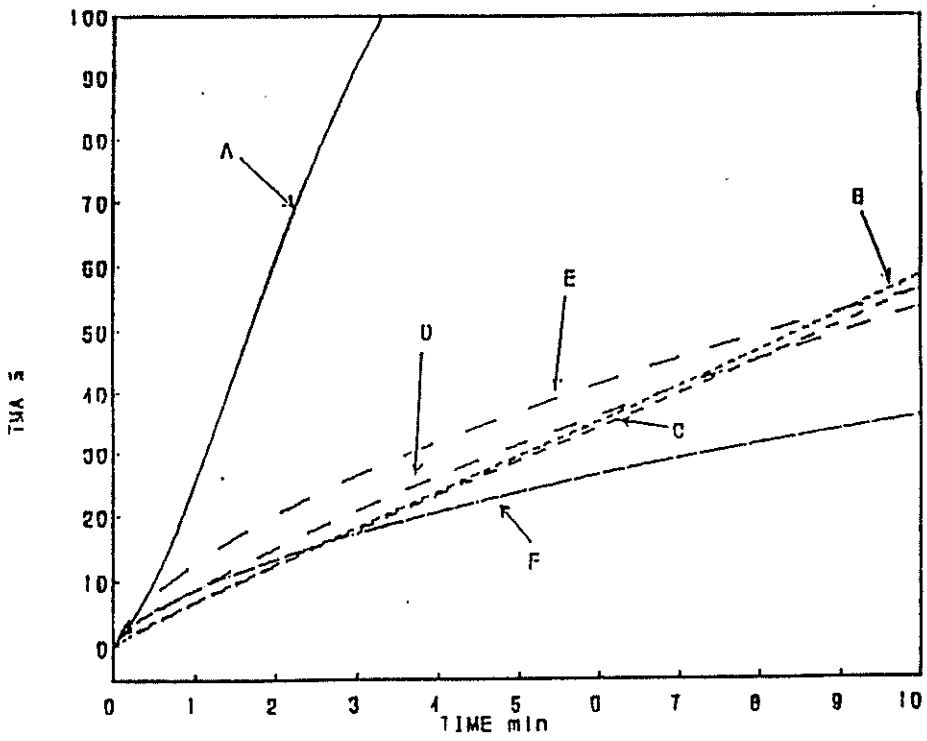

Figure 18. Shear mode creep curves of ACE/5% polymer blends: *A*, ACE; *B*, ACE/HDPE; *C*, ACE/CPEE; *D*, ACE/CPEB; *E*, ACE/CPED; *F*, ACE/CPED+1% MAH

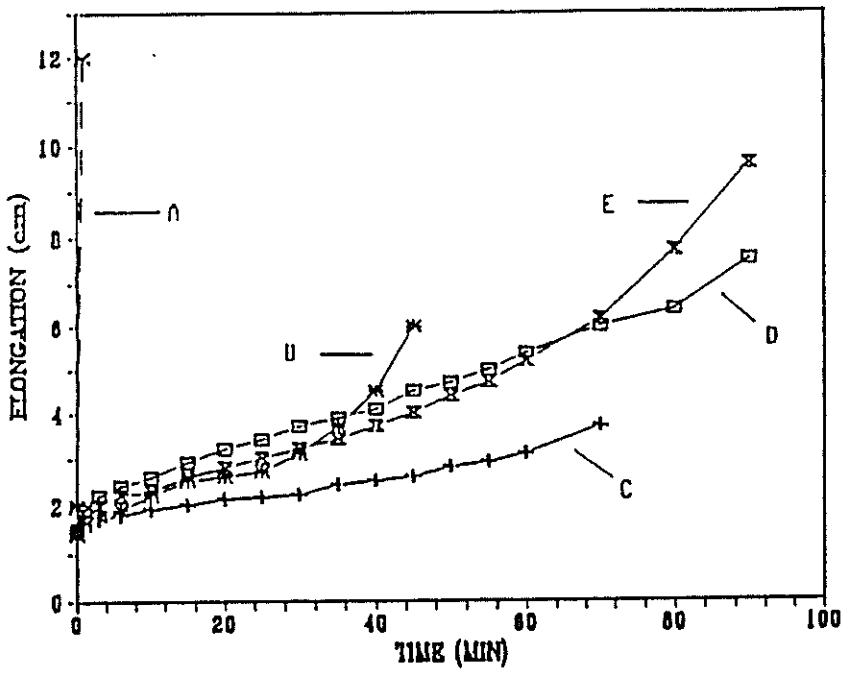

Figure 19. Tensile mode creep curves of ACE/5% polymer blends: *A*, ACE; *B*, ACE/HDPE; *C*, ACE/CPEE; *D*, ACE/CPED; *E*, ACE/CPED+1% MAH

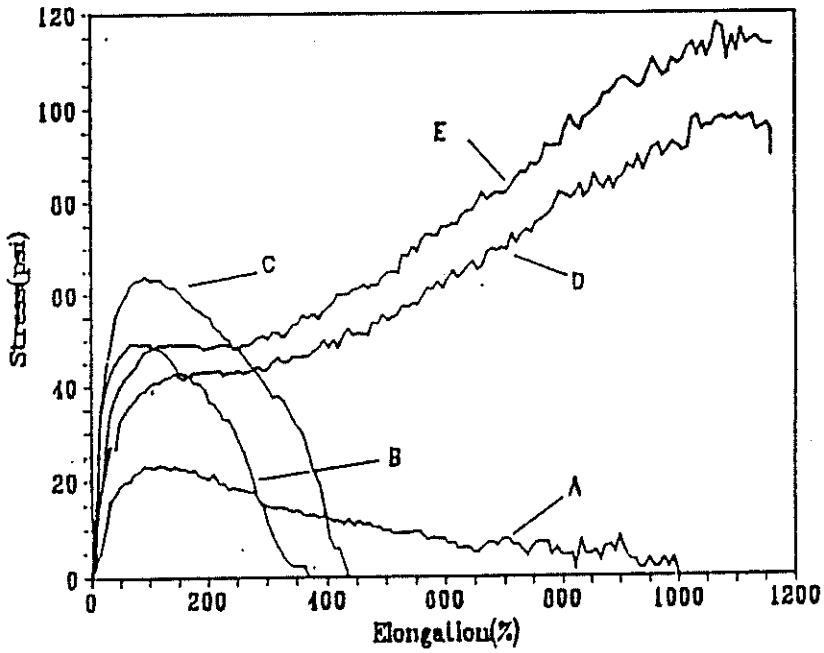

Figure 20. Stress vs. elongation plot of ACE/5% polymer blends: *A*, ACE; *B*, ACE/HDPE; *C*, ACE/CPEE; *D*, ACE/CPED; *E*, ACE/CPED+1% MAH

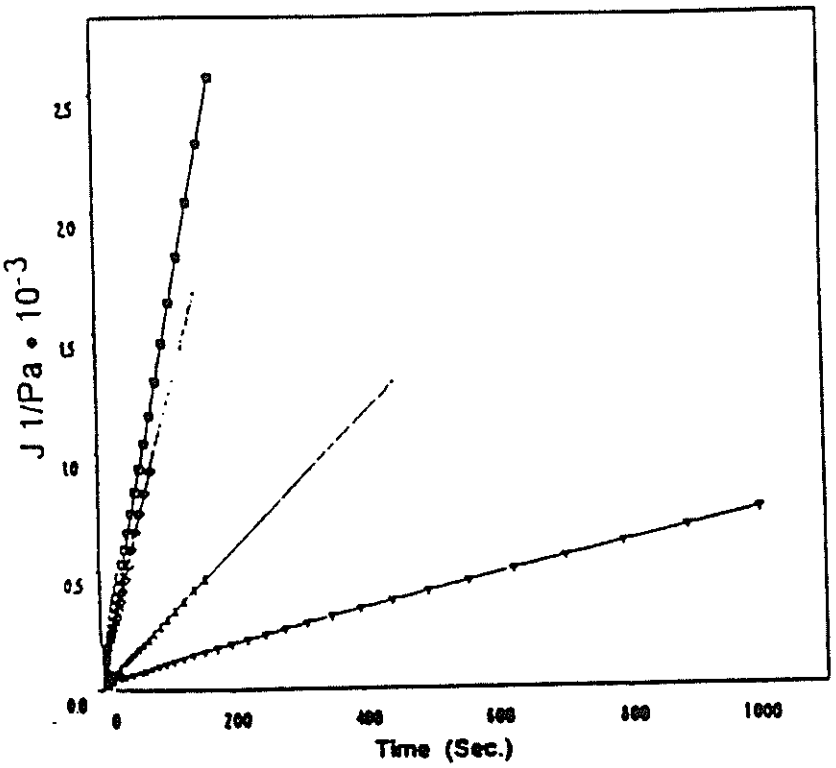

Figure 21. Constant stress creep curves at 35 °C (from top to bottom: ACD, ACD/HDPE, ACD/CPEB, ACD/CPEC)

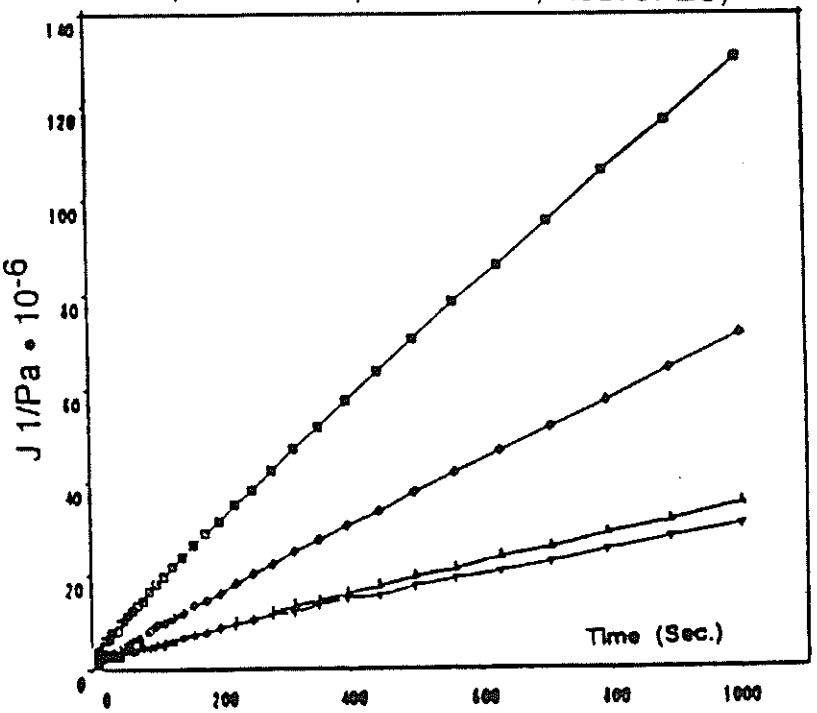

Figure 22. Constant stress creep curves at 15 °C (from top to bottom: ACD, ACD/HDPE, ACD/CPEB, ACD/CPEC)

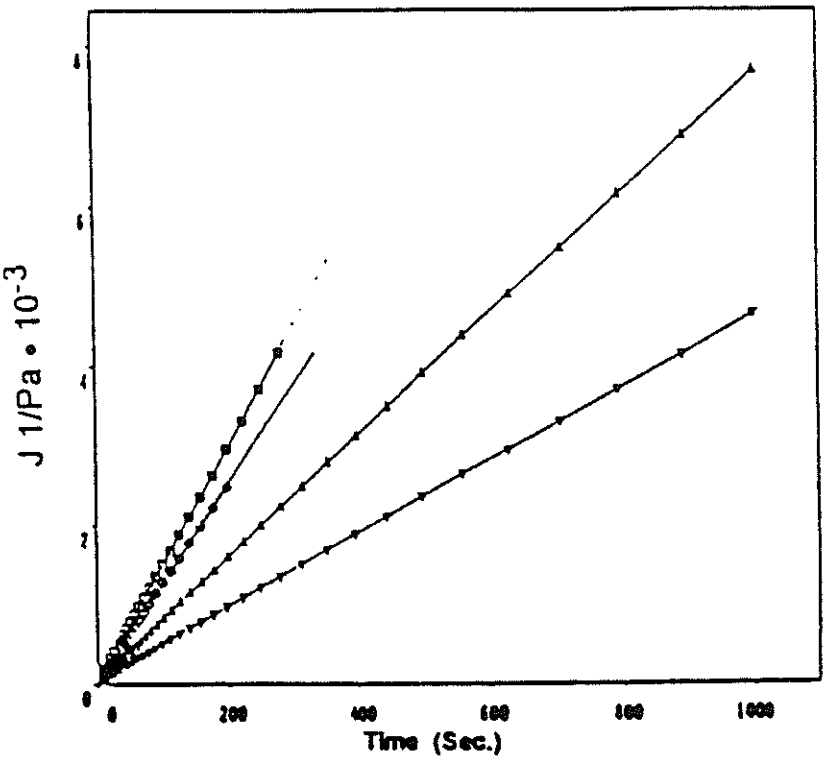

Figure 23. Constant stress creep curves at 35 °C (from top to bottom: ACE, ACE/HDPE, ACE/CPEB, ACE/CPEC)

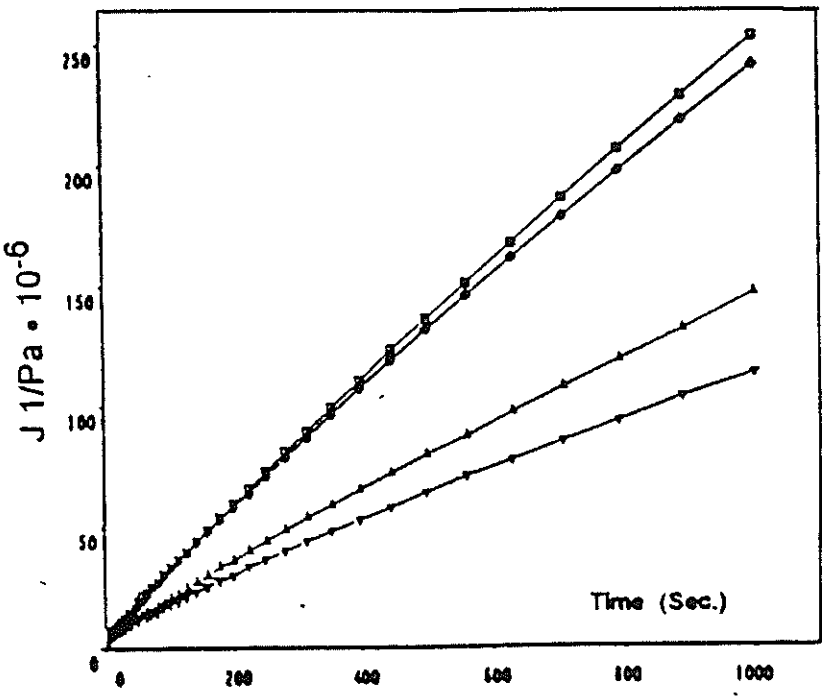

Figure 24. Constant stress creep curves at 15 °C (from top to bottom: ACE, ACE/HDPE, ACE/CPEB, ACE/CPEC)

A constant stress creep test was run at 5, 15, 25, 35°C, respectively, with a Bohlin CS rheometer using a cone and plate mode; the stress applied was 590 Pa. The tests (Figures 22-25) illustrate a pronounced difference between HDPE and CPE blends. Two different asphalt samples, ACD and ACE were blended with HDPE, semi-crystalline CPEB (8.9 wt% Cl) and amorphous CPEC (15.2 wt% Cl). With the exception of the ACE blend at 15°C, the presence of HDPE did not change the creep behavior significantly. The compliance curves observed for the HDPE blends parallel those obtained with pure asphalt. However a significant difference in the compliance of CPE blends was observed; further, one can distinguish between the degrees of chlorination in the two CPE samples. These results suggest that the more amorphous CPE samples will be more resistant to rutting.

Dynamic Mechanical Spectrometry (DMS) The DMS instruments used in this study measure the stress of a material in response to sinusoidal deformation. For an ideal elastic (Hookeian) solids, the stress will exactly follow the sinusoidal input strain. For ideal viscous (Newtonian) fluids, the stress lags 90° behind the input strain; in another words, the maximum stress will occur when the rate of strain is greatest. Between ideal elastic solids and ideal viscous fluid are viscoelastic materials. Depending on the temperature and strain frequency, the peak stress of viscoelastic materials can lag from 0° to 90° behind the applied strain.

Polymers and asphalts are viscoelastic materials which have some characteristics of both viscous fluids and elastic solids. Elastic materials have a capacity to store mechanical energy with no dissipation of energy; on the other hand, a viscous fluid has a capacity for dissipating energy, but none for storing it. When a viscoelastic material is deformed, part of the energy is stored, which is reflected in G', and part is dissipated as heat, which is reflected in G".

Rheological measurements under oscillating conditions yield the dynamic mechanical properties of polymers, i.e. the storage modulus, G', the loss modulus, G", and a mechanical damping or internal friction, tan δ. The storage modulus reflects the internal stiffness of a material under dynamic loading conditions; the corresponding

stress response is in phase with the applied strain. The loss modulus is the viscous, damped response of the material; the corresponding stress is out of phase with the applied stain. This phase lag results from the time necessary for molecular rearrangements and is associated with relaxation phenomena. In studies of the response of a material to vibrational forces, stress, strain, frequency and temperature are the key variables. When a material is subjected to cyclical stress under conditions analogous to those encountered in the intended applications, the data reflect both short-term and long-term responses to the stress conditions. If time-temperature superposition can be applied, dynamic data obtained at short time intervals at high temperature can be transformed to yield long loading time data relevant to thermal cracking [68].

Determination of Asphalt Glass Transition Temperature The glass transition temperature is a very important property to most organic materials not only because it limits practical applications but also because it can provide valuable information about the microstructure of a material. We believe that DMA is the best technique to determine T_g both in terms of accuracy and correlation with service conditions of asphalt on the road.

TABLE 9
HEAT OF FUSION (ΔH_F) OF THE ASPHALT SAMPLES

Sample	ACA	ACB	ACC	ACD	ACE	ACF	ACG	ACH
ΔH, J/g	7.7	7.8	8.5	9.2	5.8	8.6	11.3	9.6
% Cryst.	3.85	3.90	4.25	4.60	2.90	4.30	5.65	4.80
T, °C	-12	-9	-3	-5	-20	-10	0	-3

Scrutiny of Table 9 reveals that asphalts with the same grade, but from different sources, can exhibit very different T_g's. An asphalt with a higher grade may have the same or lower T_g than that of an asphalt with lower grade. The values for the activation energy of the transition process in each asphalt sample are close enough to be considered constant; an average activation energy of 9.4 kcal/mol with a standard deviation of ±0.4 kcal/mol is observed. B. Brule et. al. [44] measured T_g of four asphalt samples with DMA at eight different frequencies from 0.015 to 7.3 Hz, a lower range of

frequencies than we employed. We calculated the values for E_a from Brule's data: the results for the four samples are 9.6, 9.3, 9.3 and 8.4 kcal/mol, respectively, which are consistent with our results. The activation energy in this context is an energy barrier separating two set conformations which are in equilibrium. The height of the barrier determines the temperature dependency of wriggling rate. Thus, the constant activation energies imply that the molecular structures responsible for relaxation in each sample are the same. Previous authors [44, 69, 70] have examined fractionated asphalt samples and have shown that only saturated and aromatic fractions contribute to the glass transition. We determined the activation energy of low density polyethylene (LDPE) T_g to be 9.9 kcal/mol, which is very close to that of asphalt. Hence, we postulate that only those segments primarily composed of aliphatic units are wriggling in the glass transition process.

TABLE 10
GLASS TRANSITION TEMPERATURE (T_g) FROM E", ACTIVATION ENERGY (E_a) OF THE TRANSITION AND CRACKING TEMPERATURE (T_c) OF ASPHALTS

Asphalt	T_g °C			E_a (kcal/mol)	T_c °C
	1 Hz	10 Hz	50 Hz		
ACA	-23.0	-17.8	-13.3	9.8	-12
ACB	-24.9	-17.6	-14.5	8.8	- 9
ACC	-19.6	-17.6	-14.5	10.0	- 3
ACD	-14.9	- 9.9	- 4.1	9.4	- 5
ACE	-32.2	-26.6	-22.5	9.0	-20
ACF	-23.2	-18.8	-13.8	9.5	-10
ACG	-16.5	-10.5	- 6.1	9.7	0
ACH	-16.0	- 9.6	- 5.1	9.2	- 3

We found that imposition of a larger strain (1 %) on the asphalt samples at 50 Hz in DMA experiments will induce cracking at a specific temperature during the cooling. The temperature, called cracking temperature (T_c), can be used to estimate the low temperature cracking resistance of asphalt. The cracking temperature (T_c) is listed in Table 10. Note that all asphalt samples cracked at temperature above their T_g at 50 Hz, which implies T_g measured at this frequency can be considered the limit of

asphalt brittle temperature in the field. In five of the eight cases the asphalt sample cracked at temperature within 4°C of its T_g, however sample ACC cracked 11.5°C above its T_g. The reason behind this deviation is not clear, but we believe it is related to the morphology of the asphalt. Comparing the data on relative crystallinity of the asphalt samples with T_c (Table 10), one observes that the sample exhibiting the highest T_c is the most crystalline. There is a general inverse correlation between the extent of crystallinity and the cracking temperature.

Viscous Flow Process of Asphalt Flow curves of each asphalt sample were measured with a Bohlin CS rheometer using a cone and plate mode at temperatures ranging from 5 to 150°C. Initial Newtonian viscosities at different temperatures were determined. At temperatures well above the glass transition temperature, the viscosity is primarily governed by the energy required for a molecule to jump from one site to an adjacent site.

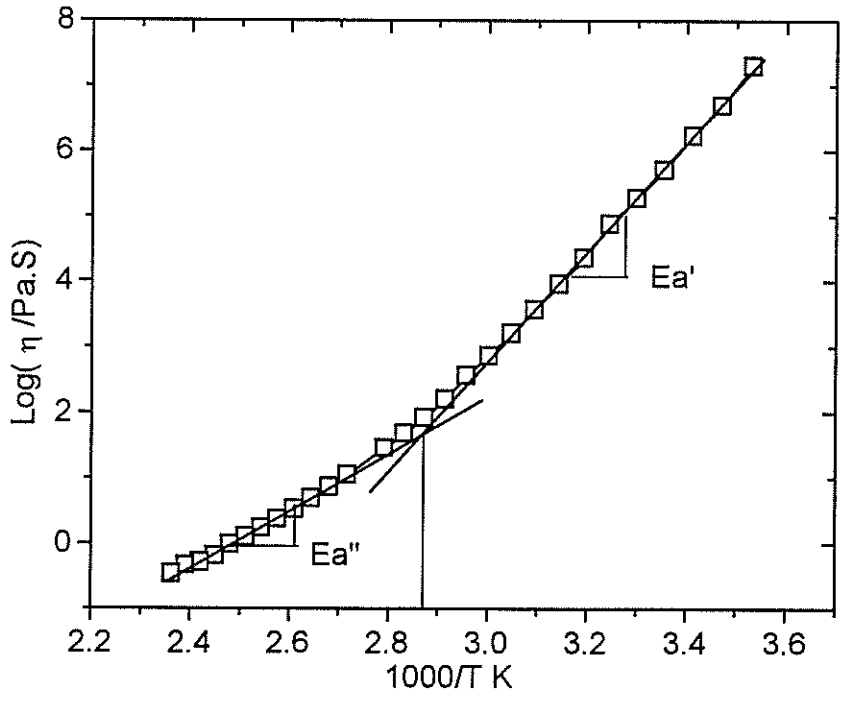

Figure 25. Arrhenius plot of the "zero" shear viscosity versus temperature for asphalt

The dependence of viscosity on temperature follows the Arrhenius equation [71]. Figure 25 is an example of the Arrhenius plot of the viscosity versus temperature for asphalt. One observes that the curve is basically comprised of two linear regions with a single inflection point. The different slopes imply that the energy barrier of the flow process changed at a certain temperature, called the onset temperature T_o, where a significant change in interaction between molecules occurred. The T_o's determined for each asphalt sample are listed in Table 11. The molecular nature of the activation energy change has not been experimentally confirmed at this point, but we speculate that dissociation of aromatic π-complexes must contribute to the change in molecular interaction. In addition, polar aromatics may interact to form of a labile three dimensional network that extends throughout asphalt; in the higher temperature regimes, the network structure dissociates.

TABLE 11

ONSET TEMPERATURE (To) IN THE ARRHENIUS PLOT OF VISCOSITY VS. TEMP.

Sample	ACA	ACB	ACC	ACD	ACE	ACF	ACG	ACH
T, °C	74	72	63	74	86	75	70	71

On a molecular basis, the magnitude of G' depends on the nature of the conformation rearrangements that can take place within the period of the deformation [72]. Examination of plots of logG' versus either temperature (Figure 26) reveals that the slope of the curve for ACE-HDPE is very close to that for ACE. In another words, adding HDPE to ACE simply induces a parallel shift of the logG' curves toward high temperature or low frequency. The presence of HDPE particles results in the development of partially separated regions in the asphalt matrix, which are characterized by a higher rigidity than in the bulk asphalt. A contributing factor to the parallel shift and the slight difference between slopes of the two curves is the selective adsorption of asphalt components by HDPE. Adsorption of the saturates by HDPE enriches the asphalt phase with aromatics resins and asphaltenes and creates a more rigid continuous phase. The dynamic mechanical response of ACE-HDPE is mainly from the continuous asphalt phase that is indirectly affected by the presence of

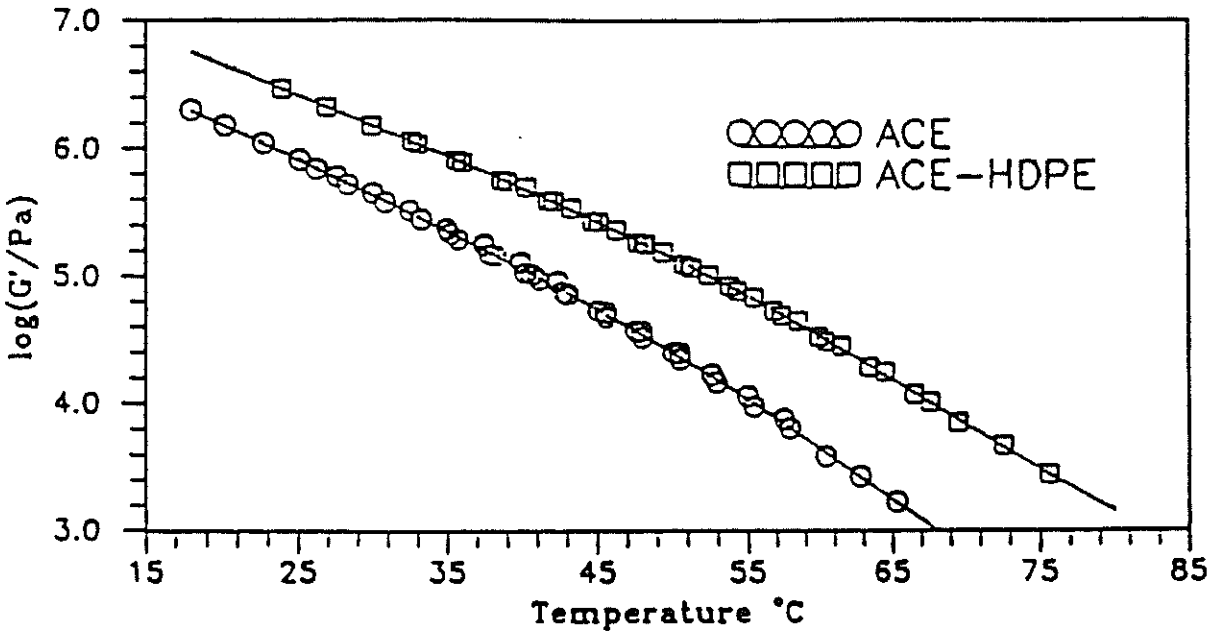

Figure 26. Plot of log G' vs. temperature for ACE and ACE/5% HDPE asphalt/polymer blends

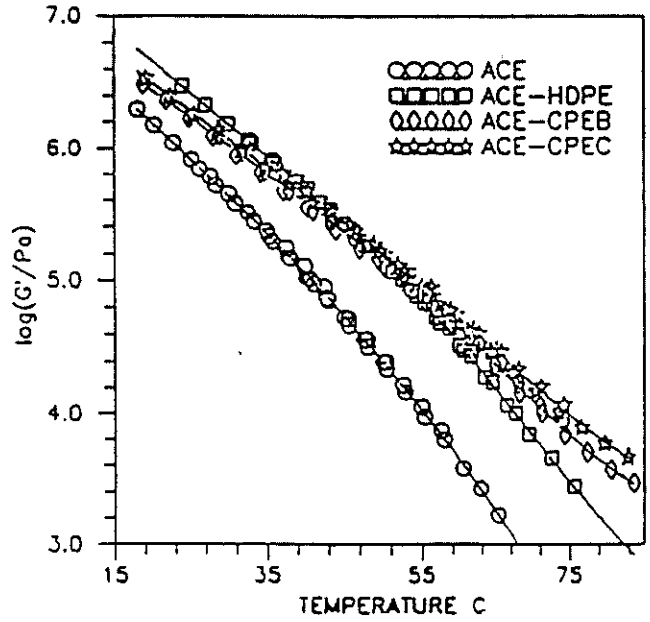

Figure 27. Plot of log G' vs. temperature for ACE, ACE/HDPE, ACE/CPEB and ACE/CPEC asphalt/polymer blends

HDPE. Compared with that of ACE/HDPE, slopes of logG' curves of ACE/CPE blends decrease and become more linear (Figure 27). Asphalt is much more temperature sensitive or frequency sensitive than the polymer additives employed. The decrease in temperature sensitivity exhibited by the blends may imply that the polymer rich phase is more and more directly involved in responding to the dynamic mechanical load. The effect is particularly pronounced in the higher temperature regimes. Introduction of chlorine atoms enhances compatibility between the polymer additives and asphalt, thus the volume of the polymer rich phase will be increased due to improved 'solubility' in the asphalt. A morphological conversion from a particle filled matrix (HDPE blend) to a three dimensional network may occur in CPE blends.

Construction of DMS Master Curves According to a temperature-time superposition principle [12, 73], data obtained at higher and lower temperatures can be equated simply and graphically with lower and higher frequencies, respectively. Conversely, data obtained at higher and lower frequency can be transposed into lower and higher temperatures, respectively.

This can be simply expressed mathematically as the following:

$$G(f1, T1) = G(f2, T2) \qquad \text{eq. 3}$$

where, G represents a mechanical property, and f and T are frequency and temperature, respectively. An example of temperature-time superposition is given in Figure 28. The figure shows the actual data points obtained over a range of temperatures and frequencies. Applying the superposition principle using a reference temperature of 40 °C, it is possible to shift each data set along the time axis to form a smooth curve called a master curve. The parameter required to shift the curves is referred to as a shift factor, a_T. A master curve in terms of temperature also can be constructed using a reference frequency of 20 Hz [37, 74] as shown in Figures 29. The superposition principle, which has been used extensively to evaluate both asphalt cements and asphalt concrete [37, 75, 76] is a powerful and convenient tool for evaluating dynamic loading data. It will help predict physical properties over wider range where direct measurements cannot be done due to instrumentation or sample limitations.

If master curves of G' and G" for a polymer blend can be constructed with only one set horizontal shift factor, a_T, this indicates that the same relaxation mechanism in G' and G" applies for both polymers, which leads to the conclusion of blend miscibility [61]. For an AC-10/polymer blend, this may show that the blend is a thermo-rheologically simple system in the temperature or frequency range. When amorphous CPE's were added, the horizontal shift was not as smooth as the others (Figure 30), so that only a "pseudomaster curve" can be constructed. The more complex rheology of these blends may imply that the polymer phase is big enough to impose a second relaxation mechanism on the asphalt continuous phase.

Strength of Polymer Modified Asphalt Although extensive data can be acquired using dynamic mechanical analysis, DMA, selection of the correct parameters in the data analysis for predicting service performance of asphalt binders is not immediately obvious. G^*, the ratio of the peak stress to the peak strain, reflects the total stiffness. The in-phase component of $|G^*|$ is the shear *storage modulus, G'*, and represents the part of the input energy which is not lost to heat (the elastic portion). In the SHRP specifications, the resistance of the asphalt binder to fatigue cracking is considered by specifying a maximum value for the stiffness parameter $G^* \sin \delta$ at the average pavement design temperature [77 78]. Since by definition $\sin \delta = G''/G^*$, it follows that $G^* \sin \delta = G''$, the shear *loss modulus,* implying that the loss modulus is indicative of this pavement distress. This parameter relates the contribution of the asphalt binder to the dissipation of energy in a pavement during each loading cycle. Since the loss modulus is a measure of the viscous flow within a viscoelastic fluid, this parameter relates also to permanent deformation at high temperatures. King et al. [79] demonstrated that G'' does indeed correlate quite well with results from the rutting simulator. Below certain values at the test temperature, there was an approximately linear relationship of rut depth to $\log(G'')$. A similar correlation between rutting resistance and $G^*/\sin \delta$ was anticipated by SHRP investigators.

The polymeric additives increase the storage modulus of the asphalt mixes by an order of magnitude at lower frequencies and with the exception of HDPE mixes the

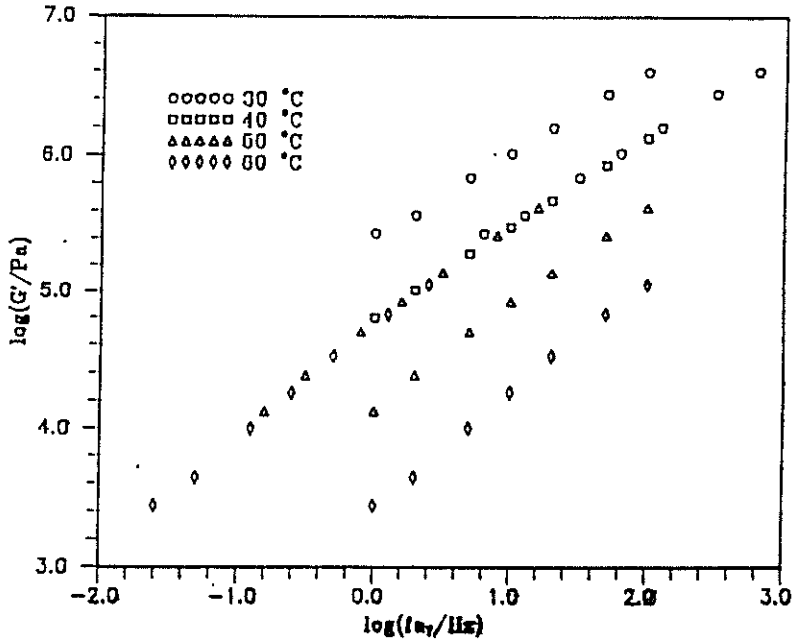

Figure 28. *G'* reduced frequency master curve for ACE/HDPE blend; reference temperature = 40 °C

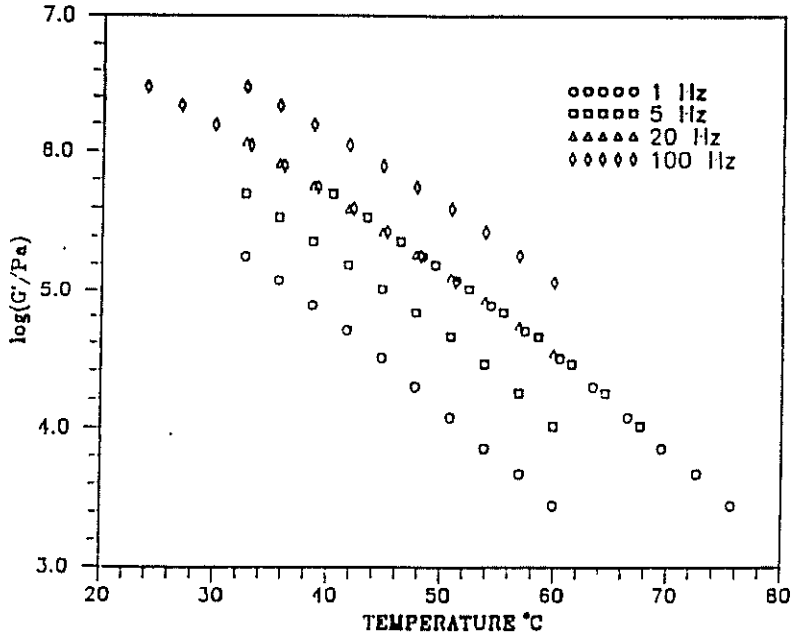

Figure 29. *G'* reduced temperature master curve for ACE/HDPE blend; reference frequency = 20 Hz

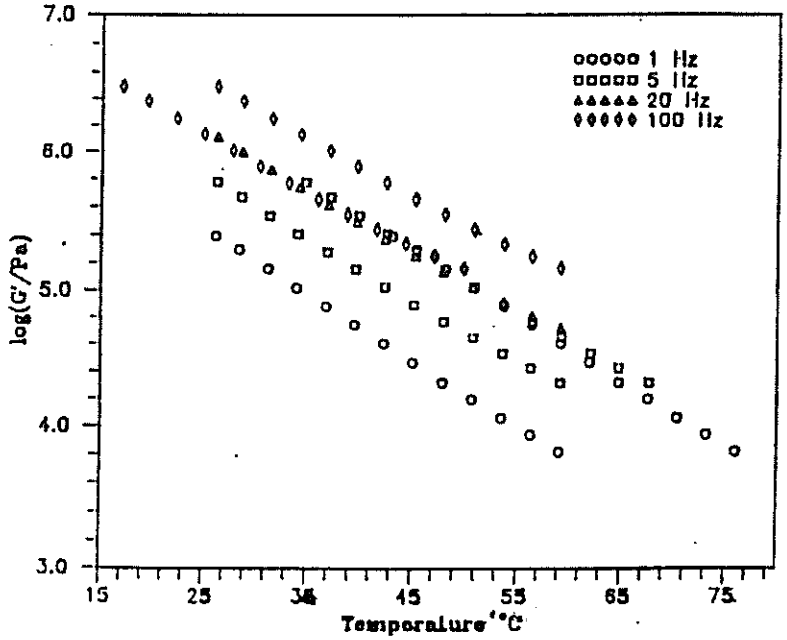

Figure 30. *G'* reduced temperature master curve for ACE/CPEC; reference frequency = 20 Hz

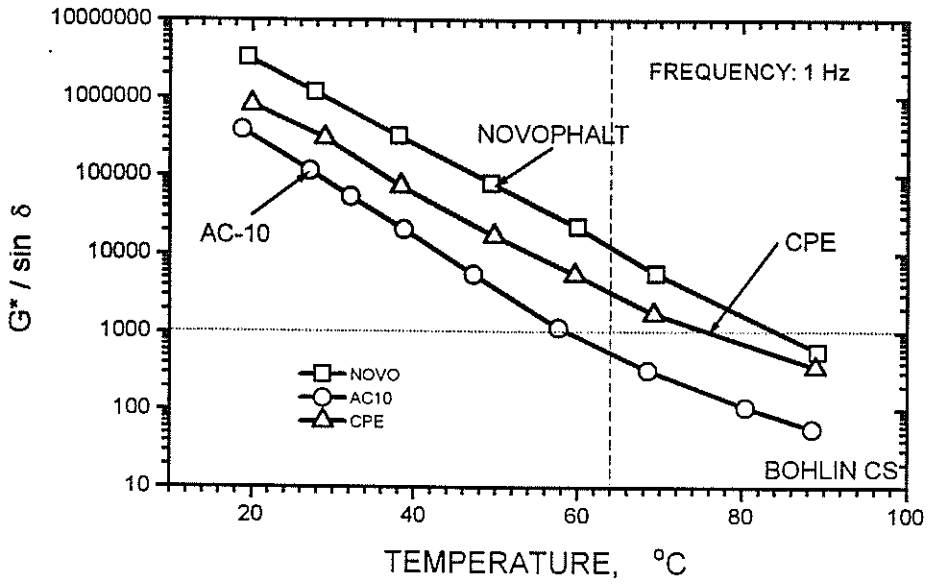

Figure 31. Isochronal plots of G*/sin δ for neat and polymer modified paving grade AC-10 binders. Reference material: NOVOPHALT AC-10

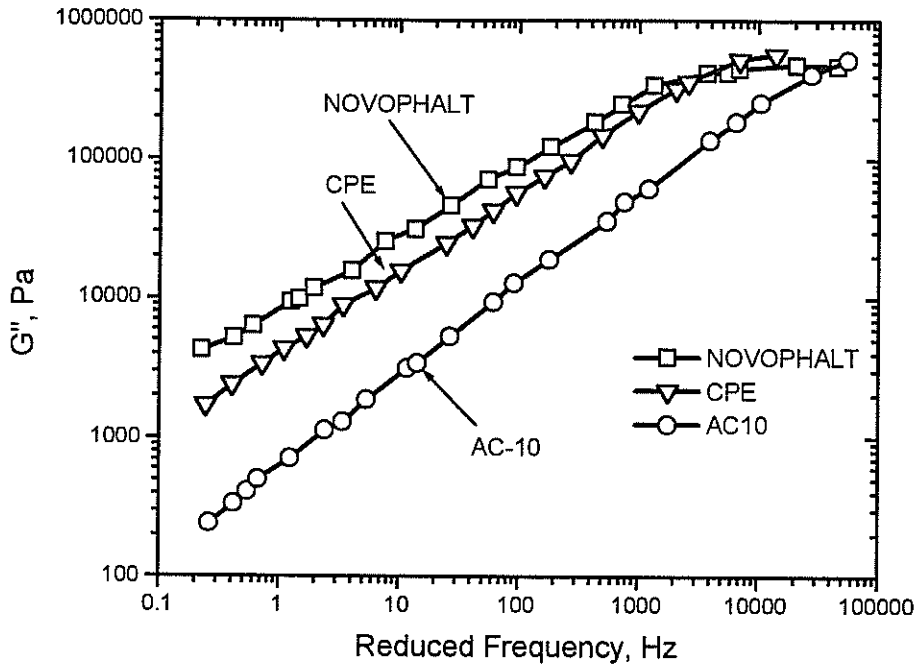

Figure 32. Plots of shear loss modulus, *G"*, versus reduced frequency of neat and polymer/ AC-10 C binders. Reference material: NOVOPHALT AC-10

temperature susceptibility is decreased. This is apparent from the slope of the isochronal plots of G*/sin δ vs. temperature (Figure 31). The impact of polymeric additives on the loss modulus is illustrated by a plot of G" vs. reduced frequency shown in Figure 32. A commercial PMAC, Novophalt, is also included in both plots. At low frequencies, corresponding to high temperatures, the higher viscosities of the PMAC's is apparent, particularly with the HDPE mix. Chlorination of the HDPE reduced the high temperature G" and produced a mix quite comparable to Novophalt.

Two pairs of AC-10/CPE blends were selected to investigate the influence of chlorine distribution. Pair A is AC-10/CPEB and AC-10/CPEE (CPE's with low chlorine contents), and pair B is AC-10/CPEC and AC-10/CPEF (CPE's with moderate chlorine contents). CPEB and CPEC were chlorinated in solution to favor a random chlorine distribution, and CPEE and CPEF were prepared under heterogeneous conditions to produce a chain structure similar to block copolymer. In Figures 33 and 34, the

temperature dependence of the absolute value of the complex moduli, G^* of pairs A and B are shown, respectively, with AC-10 and AC-10/HDPE as references. It is apparent that all AC-10/CPE blends are less temperature sensitive than AC/HDPE and AC-10; furthermore, pair A is less temperature sensitive than pair B.

Tan δ of viscoelastic material is a ratio of dissipated energy in its viscous component to stored energy in its elastic component in a cyclic deformation. It seems, therefore, that the more elastic, the smaller the tan δ. This is only true when the temperature is above glass transition temperature of material and close to its softening point, and also when the material is not crosslinked. If no crosslinks are present, the energy is dissipated through slippage of the whole molecular chain, which in turn leads to permanent deformation. Since asphalts and polymer modified asphalts are not three dimensionally crosslinked materials and the experimental temperature range in this study is also close to the softening point of the materials, tan δ can be used to indicate relative elasticity or the contribution of elastic component to strength of the asphalt-polymer blends. Figure 35 shows the contribution of elastic component increases with

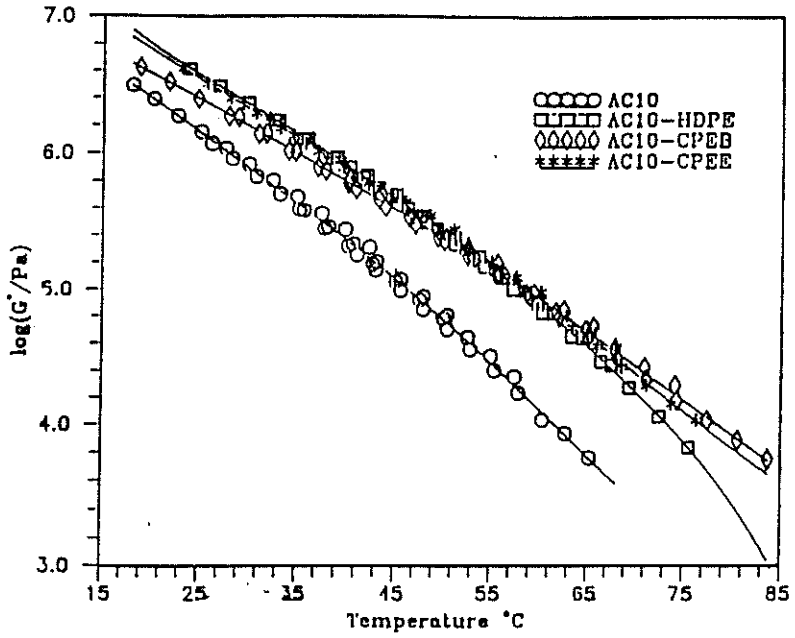

Figure 33. Plot of logG* vs. temperature for ACE, ACE/HDPE, and CPE pair A (ACE/CPEB and ACE/CPEE)

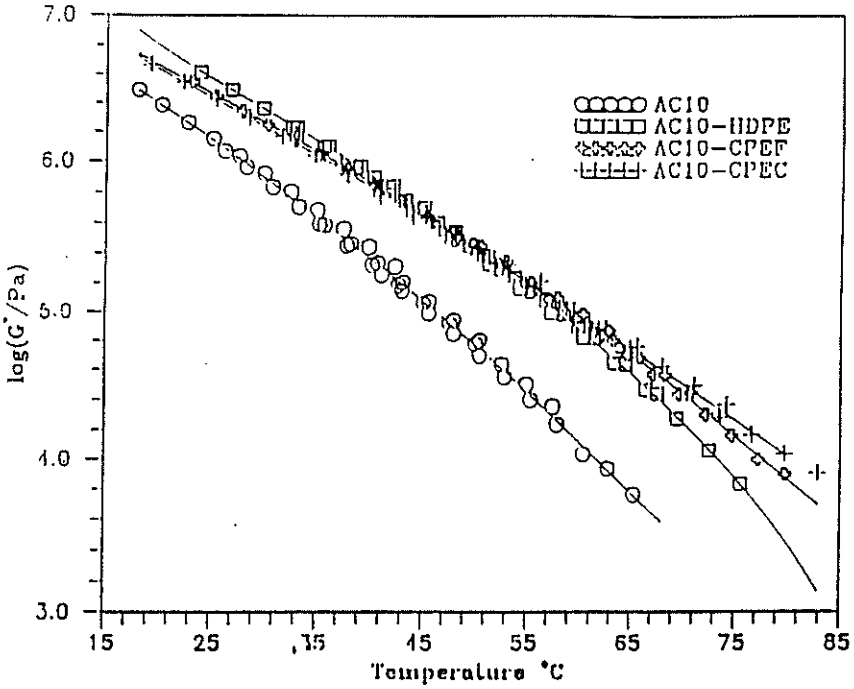

Figure 34. Plot of logG* vs. temperature for ACE, ACE/HDPE, and CPE pair B (ACE/CPEC and ACE/CPEF)

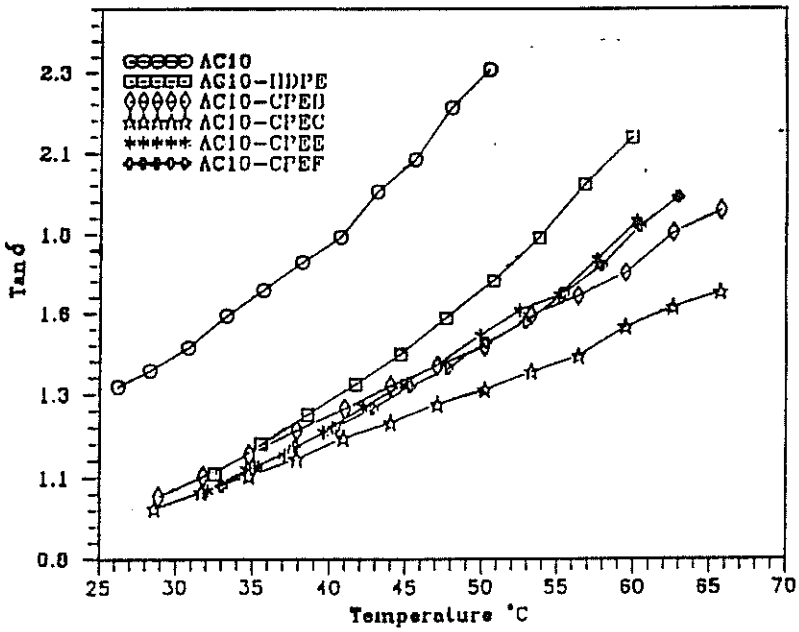

Figure 35. Plot of tan δ vs. temperature for ACE, ACE/HDPE, ACE/CPEB, ACE/CPEE, ACE/CPEC, and ACE/CPEF

chlorine content for blends of AC-10 and homogeneously prepared CPE's. Tan δ's of the two blends of homogeneously chlorinated CPE's are quite close. Tan δ of ACE/CPEC containing homogeneously prepared CPE is considerably lower than that of ACE/CPEF containing heterogeneously prepared CPE. The residual crystalline regions in the CPE with a non-random distribution of chlorine atoms act as fillers and harden the asphalt/CPE blends.

Low temperature cracking The low temperature cracking test is quite sensitive to polymer/asphalt interactions. Since asphalt is a rather low molecular weight material, it becomes quite brittle at temperatures below its glass transition. In contrast, the T_g's of HDPE and CPE are greater than 30°C below the cracking temperatures of the blends. The amorphous regions of these polymers remain flexible while the crystalline phases provide tie points to limit chain reptation. Thus, these polymers should be effective impact modifiers. However, the extent of polymer contribution to blend properties depends upon the degree of compatibility with the asphalt matrix.

TABLE 12

GLASS TRANSITION TEMPERATURE (T_g) FROM E" AND CRACKING TEMPERATURE (T_c) OF CONCERNED ASPHALTS, POLYMERS AND ASPHALT/POLYMER BLENDS

Sample	T_g°C			T_c°C
	1 Hz	10 Hz	50 Hz	
ACE	-32.2	-26.6	-22.5	-20
ACD	-14.9	- 9.9	- 4.1	- 5
CPEB	-12.7	- 7.9	- 5.7	
CPEC	-15.2	-12.4	- 9.4	
ACE/HDPE	-30.3	-25.0	-20.5	-23
ACE/CPEB	-31.9	-26.3	-21.6	-28
ACE/CPEC	-31.8	-25.7	-21.4	-31
ACD/HDPE	-14.3	- 8.5	- 3.7	- 7
ACD/CPEB	-16.9	-10.8	- 6.0	- 8
ACD/CPEC	-16.6	-10.4	- 6.7	- 10

As can be seen in Table 12, the blends do indeed exhibit T_c's below the T_g of pure asphalt measured at the same frequency. We have shown that the T_c of pure asphalt falls above the corresponding T_g so the polymer component has improved the

low temperature properties of the blends. Furthermore, CPE modified asphalts have lower T_c's than HDPE modified asphalts as might be expected from a more amorphous polymer with a higher degree of interaction with asphalt. Thus, our data indicate that CPE's are more compatible with asphalt than HDPE and are more effective in low temperature reinforcement.

The enhanced compatibility of CPE in asphalt can be attributed to a change in the polymer polarity as well as changes in morphology stemming from the reduced crystallinity. In crystalline polymers like HDPE, interaction with solvents and reagents is limited to the readily accessible amorphous regions. In HDPE, these regions are composed of $-CH_2-$ segments more compatible with the saturates in asphalt. One would expect selective extraction of the saturates from the asphalt matrix by HDPE; this process would disrupt the balance of components in asphalt mixtures and promote phase separation.

CONCLUSIONS

1. Low level chlorination of polyethylene can be controlled to produce semicrystalline polymeric additives. The chlorine distribution with the polymer molecule is not random; blocks of crystalline polyethylene segments remain dispersed in amorphous chlorinated segments. Chlorinated polyethylenes containing less than 15 wt% chlorine interact more extensively with an asphalt matrix than polyethylene. The interaction is substantiated by changes in the DSC, creep resistance and blend rheology.

2. Differential scanning calorimetry can be used to ascertain the thermal transitions in asphalt samples. In general, two low temperature relaxations, a glass transition and a melting point can be identified in pure asphalt samples. The magnitude of the transitions varies proportionally to the distribution of asphalt components among phases in asphalt-polymer blends. No asphalt melting point is detected in polyethylene blends and the low temperature transitions are diminished. In contrast, CPE blends enhance the magnitude of the low temperature transitions and the asphalt melting point can still be detected in blends containing less than 10 wt% polymer. We believe that CPE are less disruptive to the balance of asphalt components than polyethylene and that more stable blends can be produced.

3. Dynamic mechanical spectroscopy is the most accurate technique for measuring asphalt glass transitions, which can be correlated with low temperature cracking. The glass transition is frequency dependent so measurements at 50 Hz are the most useful because this condition duplicates the oscillations generated by vehicular traffic. The glass transition temperatures in the samples evaluated ranged from -22.5°C to -4.1°C; however, the activation energy for the process was constant at 9.4 kcal/mol. The corresponding activation energy for the T_g of polyethylene is 9.9 kcal/mol. The similarity suggests that the amorphous aliphatic components of asphalt control the T_g of asphalts. The low temperature cracking properties of asphalts closely parallel the T_g's measured at 50 Hz. Both the T_g and low temperature cracking temperatures increase when the crystalline asphalt component increases.

4. Dynamic mechanical analysis of asphalt-blends reveals the loss modulus, G', the storage modulus, G", and internal friction, tan δ. Asphalt-polyethylene blends are more rigid than asphalt but the temperature sensitivities are parallel. Asphalt-CPE blends are less temperature sensitive and the temperature sensitivity varies inversely with the CPE chlorine content. A morphological conversion from a particle filled matrix (HDPE blend) to a continuous polymer phase may occur in CPE blends at proper polymer concentrations. The decrease in temperature sensitivity observed implies that the polymer rich phase is responding more directly in CPE blends.

5. A constant stress creep test is a very sensitive method for detecting asphalt-polymer interaction. At 5% loading, HDPE did not change the creep behavior of asphalt substantially. The compliance curves observed for the HDPE blends parallel those obtained with pure asphalt. However, a significant difference in the compliance of CPE blends is observed; further, one can distinguish between degrees of chlorination in the CPE additive. This test may be the best indicator of rutting resistance of asphalt cements in the field.

REFERENCES

1. *The Asphalt Handbook*, Asphalt Institute, Manual Series No. 4 (MS-4), College Park, MD, 1989, p. 7.
2. Halstead, W. J., Proceedings of the Association of Asphalt Paving Technologists, Vol. 54, 1985, pp. 91-117.
3. Peterson, J. C., Transportation Research Record, No. 999, 1985, pp. 13-30.
4. Corbett, L. W., Analytical Chemistry, Vol. 41(4), 1969, pp. 576-9.
5. Tuffour, Y.A. et al., Proceedings of the Association of Asphalt Paving Technologists, Vol. 58, 1989, pp. 163-181.
6. Brule, B., Ramond, R., and Such, C., Transportation Research Record, No. 1096,1986, pp. 22-34.
7. Mahboub, K., Journal of Testing and Evaluation, Vol. 18, 1990, p. 210.
8. Elliot, R. P. and Herrin, M., Proceedings of the Association of Asphalt Paving Technologists, Vol. 54, 1985, pp. 209-237.
9. Valkering, C. P. and Van Gooswillingen, G., Proceedings of the Association of Asphalt Paving Technologists, Vol. 58, 1989, pp. 238-255.
10. Finn, F. N. et al, National Cooperative Highway Research Program Report No. 195, Transportation Research Board, Washington, D.C. 1978.
11. Glover, C. J., et. al., Research Report No. 419-1F, Texas Transportation Institute, May 1987.
12. Malan, G. W. et al., Proceedings of the Association of Asphalt Paving Technologists, Vol. 58, 1989, pp. 142-162.
13. Edler, A.C. et al., Proceedings of the Association of Asphalt Paving Technologists, Vol. 54, 1985, pp. 118-139.
14. Hailey, D., Highway and Heavy Construction, March, 1987, pp. 42-43.
15. Tahmoress, M., Romine, R. A., and Gainer, A. B., Strategic Highway Research Program A-004 Report, March 1991.
16. Stewart, L., Highway and Heavy Construction, December, 1989, pp. 48-50.
17. King, G. N., Muncy, H. W. and Prudhomme, J.B., Proceedings of the Association of Asphalt Paving Technologists, Vol. 55, 1986, pp. 519-540.

18. Terrel, R. L. and Walter, J. L., Proceedings of the Association of Asphalt Paving Technologists, Vol. 55, 1986, pp. 482-518.
19. Collins, J. H. and Mikols, W. J., Proceedings of the Association of Asphalt Paving Technologists, Vol. 54, 1985, pp. 1-17.
20. Khosla, N., Zahran, S. Z. and Zahran, P., Proceedings of the Association of Asphalt Paving Technologists, Vol. 58, 1989, 274-302.
21. Strommer, E., U. S. Patent No. 4,617,220, 14 Oct. 1986.
22. Uchida, M. and Jinno, S., Jpn Kokai Tokkyo Koho JP 62 275,160, Nov. 1987, Chemical Abstracts, 108:191717, 1988.
23. Nakabayashi, H., Hayashi; K., Taniguchi, K., Shimizu, Y., Jpn Tokkyo Koho JP 61 152,764, Jan., 1986; Chemical Abstracts, 106:22419, 1987.
24. Kao Corp., Jpn Kokai Tokkyo Koho JP 60 01,260, Jan., 1985, Chemical Abstracts, 103:41640, 1985.
25. Kovalev, Y. N. ; Busel, A. V., Akulich, A. V., USSR. SU 1,104,143, Jul., 1984, Chemical Abstracts, 101:215567, 1984.
26. Nippon Oil Co., Ltd., Jpn Kokai Tokkyo Koho JP 57 87,461, May, 1982, Chemical Abstracts, 97:184130, 1982.
27. Miyazaki, Y., Jpn Kokai Tokkyo Koho JP 54 155,218, Dec., 1979, Chemical Abstracts, 92:148693, 1980.
28. Yonekura, K. Fujika, K., Jpn Kokai Tokkyo Koho JP 51 14,937, Feb., 1976, Chemical Abstracts, 85:7056, 1976.
29. Kloboucek, B., Cermak, B., Matetju, K., Zurek, A., Czech. CS 208,029, Oct., 1982, Chemical Abstracts, 98:184640, 1983.
30. Podolan, J., Czech. CS 234,856, Jan., 1987, Chemical Abstracts, 106:200911, 1987.
31. Button, J. W., Little, D. N., Kim, Y., Ahmed, J., Proceedings of the Association of Asphalt Paving Technologists, Vol. 56, 1987, 62-90.
32. Jew, P. and Woodhams, R.T., Proceedings of the Association of Asphalt Paving Technologists, Vol. 55, 1986, pp. 541-559.
33. Winkler, D.S., U. S. Patent No. 4,818,367, 4 Apr. 1989.

34. Coyne, L. D., Proceedings of the Association of Asphalt Paving Technologists, Vol. 57, 1988, pp. 545-575.
35. Brule, B., Brion, Y., Tanguy, A., Proceedings of the Association of Asphalt Paving Technologists, Vol. 57, 1988, pp. 41-64.
36. Highway and Heavy Construction, Vol. 131, 1988, pp. 56-57.
37. Goodrich, J. L., Proceedings of the Association of Asphalt Paving Technologists, Vol. 57, 1988, pp. 116-175.
38. Heukelom, W., Proceedings of the Association of Asphalt Paving Technologists, Vol. 42, 1973, p. 67.
39. Heukelom, W., Journal de l' Institute du Petrole, Vol. 55, 1969, pp. 404-417.
40. L. Petrakis, D.T. Allen, G.R. Gavalas and B.C. Gates, Analytical Chemistry, Vol. 55, Aug. 1983, pp. 1557-1564.
41. Peterson, J. C., Transportation Research Record, Vol. 1096,1986, p. 1.
42. Cookson, D. J. and Smith, B., Journal of Magnetic Resonance, 57, 1984, p. 355.
43 Noel, F. and Corbett, L. W., Journal de l' Institute du Petrole, Vol. 56, 1970, p. 261.
44 Brule, B., Planche, J. P., King, G., P. Claudy, P., Letoffe, J. M., Preprints of the American Chemical Society, Division of Petroleum Chemistry, Vol. 35(3), 1990, pp. 330-337.
45. Hesp, S. A. and Woodhams, R. T., in *Polyolefin-Asphalt Emulsions*, Wardlaw, K. R. and Schuler, S., Eds., ASTM STP 1108, Philadelphia, PA, 1991.
46. Pitchford, A. C. and Sarret, H. J., U.S. Patent No. 3,312,649, Apr. 1967.
47. Fogg, S. G. and Westerman, P. H., British Patent No. 1,475,924, Jun. 1977.
48. Quenum; B. M., Berticat, P., Vallet, G., Polymer Journal, Vol.7(3), 1975, pp. 300-311.
49. Abu-isa, I. A. and Myers, Jr., M. E. , Journal of Polymer Science: Polymer Chemistry Edition, Vol. 11, 1975, pp. 225-231.
50. Bikson; B., Jagur-Grodzinski, J., Vofsi, D., Organic Coatings and Plastics Chemistry, Vol. 45, 1981, pp. 257-262.

51. Brame, Jr., E. G., Journal of Polymer Science: Part A-1, Vol. 9, 1971, pp. 2051-2061.
52. Chai; Z., Shi, L., Sheppard, R. N., Polymer, Vol. 25, 1984, pp. 369-374.
53. Chang; B. H., Zeigler, R., Hiltner, A., Polymer Engineering and Science, Vol. 28(18), 1988, pp. 1167-1181.
54. Krimm, S., Pure and Applied Chemistry, Vol. 16, 1969, p. 369.
55. Harrison, I. R. and Baer, E., Journal of Polymer Science: Part A-2, Vol. 9, 1971, p. 1305.
56. Era, V. A., Makromolekulare Chemie, Vol. 167, 1973, p. 321.
57. Bikson; B., Jagur; J., Vofsi, D., Journal of Polymer Science: Polymer Physics Edition, Vol. 19, 1981, p. 361.
58. Biegenzein, G., U.S. Patent No. 4,314,921, 9 Feb. 1982.
59. Montgomery, D. P., U.S. Patent No. 3,547, 850, 15 Dec.1970.
60. Peterson; J. C., Plancher; H., Harnsbereger, P.M., Proceedings of the Association of Asphalt Paving Technologists, Vol. 56, 1987, pp. 632-649.
61. Utracki, L. A., *Polymer Alloys and Blends*, Hanser, New York, 1990, p. 22.
62. Wendlandt, W. W. and Gallagher, P. K., in *Thermal Characterization of Polymeric Materials,* Edith A. Turi, Editor, Academic Press, New York, 1981, Chapter 1.
63. Flory, P. J., *Principles of Polymer Chemistry*, Cornell University Press, Ithaca, NY, 1962.
64. Lenoble, C., Preprints of the American Chemical Society, Division of Petroleum Chemistry, Vol. 35(3), 1990, pp. 541-549.
65. Collins, J. H., Bouldin, M. G., Gelles, R., Berker, A., Proceedings of the Association of Asphalt Paving Technologists, Vol. 60, 1991, 43-79.
66. Bucknall, C. B. and Stevens, W. W., Journal of Materials Science, Vol. 15, 1990, p. 2950.
67. Bucknall, C. B. and Page, C. J., Journal of Materials Science, Vol. 17, 1992, p. 808.

68. Pink, H. S., Merz, R.E., Bosniack, D. S Proceedings of the Association of Asphalt Paving Technologists, Vol. 49, 1980, pp. 64-94.

69 Wada, Y. and Hirose, H., Journal of Applied Physics, Japan, Vol. 30, 1961, p. 40.

70 Huynh, H. K., Khong, T. D., Malhotra, S. L., Blanchand, L. P., Analytical Chemistry, Vol. 50(7), 1978, p. 978.

71 Vinogradov, G. V. and Malkin, A. Y., *Rheology of Polymers,* Mir Publishers, Moscow, 1980, p. 105.

72. Bird, R. B., Armstrong, R. C., Hassager, O., *Dynamics of Polymeric Liquids, Volume 1, Fluid Mechanics,* 2nd Edition, John Wiley & Sons, Inc., New York, 1987.

73. Ferry, J. D., *Viscoelastic Properties of Polymers*, 3rd Edition, John Wiley & Sons, Inc., New York, 1980.

74. Shoham, E. and Eisenberg, A., ., Journal of Polymer Science: Polymer Physics Edition, Vol. 14, 1976, pp. 1211-1212.

75. Monismith, C. L., Alexander, R. L., Secor, K. E., Proceedings of the Association of Asphalt Paving Technologists, Vol. 35, 1966, pp. 400-450.

76. Schmidt, R. J., Transportation Research Record No. 544, 1975.

77. Anderson, D. A., Christensen, D. W., Bahia, H., Proceedings of the Association of Asphalt Paving Technologists, Vol. 60, 1991, pp. 437-532.

78. Christensen, D. W., Anderson, D.A., Proceedings of the Association of Asphalt Paving Technologists, Vol. 61, 1992, 67-116.

79. King, G.N., King, H.W., Harders, O., Chavenot, P., Planche, J-P., Proceedings of the Association of Asphalt Paving Technologists, Vol. 61, 1992, 29-66.

This public document is published at a total cost of $1072.00. Two hundred twenty-five copies of this public document were published in this first printing at a cost of $654.00. The total cost of all printings of this document including reprints is $1072.00. This document was published by Louisiana State University, Graphic Services, 355 River Road, Baton Rouge, Louisiana 70802, to report and publish research findings of the Louisiana Transportation Research Center as required in R.S. 48:105. This material was printed in accordance with standards for printing by state agencies established pursuant to R.S. 43:31. Printing of this material was purchased in accordance with the provisions of Title 43 of the Louisiana Revised Statutes.